Representing potential energy surfaces by high-dimensional neural network potentials

2014 J. Phys.: Condens. Matter 26 183001

(http://iopscience.iop.org/0953-8984/26/18/183001)

IOP Publishing Journal of Physics: Condensed Matter

J. Phys.: Condens. Matter **26** (2014) 183001 (24pp) doi:10.1088/0953-8984/26/18/183001

Topical Review

Representing potential energy surfaces by high-dimensional neural network potentials

J Behler

Lehrstuhl für Theoretische Chemie, Ruhr-Universität Bochum, D-44780 Bochum, Germany

E-mail: joerg.behler@theochem.rub.de

Received 19 January 2014
Accepted for publication 27 February 2014
Published 22 April 2014

Abstract

The development of interatomic potentials employing artificial neural networks has seen tremendous progress in recent years. While until recently the applicability of neural network potentials (NNPs) has been restricted to low-dimensional systems, this limitation has now been overcome and high-dimensional NNPs can be used in large-scale molecular dynamics simulations of thousands of atoms. NNPs are constructed by adjusting a set of parameters using data from electronic structure calculations, and in many cases energies and forces can be obtained with very high accuracy. Therefore, NNP-based simulation results are often very close to those gained by a direct application of first-principles methods. In this review, the basic methodology of high-dimensional NNPs will be presented with a special focus on the scope and the remaining limitations of this approach. The development of NNPs requires substantial computational effort as typically thousands of reference calculations are required. Still, if the problem to be studied involves very large systems or long simulation times this overhead is regained quickly. Further, the method is still limited to systems containing about three or four chemical elements due to the rapidly increasing complexity of the configuration space, although many atoms of each species can be present. Due to the ability of NNPs to describe even extremely complex atomic configurations with excellent accuracy irrespective of the nature of the atomic interactions, they represent a general and therefore widely applicable technique, e.g. for addressing problems in materials science, for investigating properties of interfaces, and for studying solvation processes.

Keywords: interatomic potentials, neural networks, molecular dynamics

(Some figures may appear in colour only in the online journal)

1. Introduction

In recent years computer simulations have become a powerful tool for gaining atomic-scale insights into a wide range of chemical processes, from biochemistry to materials science. Using the broad spectrum of available theoretical methods, valuable information can be obtained giving a detailed understanding of experimental results. Even data not accessible at all to experiment can be obtained.

A mandatory condition for carrying out computer simulations using state-of-the-art molecular dynamics (MD) [1, 2] or Monte Carlo (MC) [3, 4] methods is the availability of reliable energies (and forces) for a large number of atomic configurations. For systems of moderate size with up to a few hundred atoms, it is possible to use electronic structure methods on-the-fly. In particular, for MD this has become a well-established technique and such *ab initio* MD [5, 6] simulations have been applied with great success to many interesting problems in chemistry and condensed matter physics. To date, density-functional theory (DFT) [7, 8] is the dominant electronic structure method in the field of *ab initio* MD, since the application of higher-level wave function-based methods is too demanding even if powerful supercomputers are available. Still, even when using DFT, which offers a good compromise between accuracy and efficiency for many systems, the accessible simulation times remain too short and the number

of atoms that can be included is too small to address many interesting problems.

A common approach for determining the energies and forces in large-scale simulations is to replace computationally demanding electronic structure calculations by more efficient potentials. For this purpose many different techniques have been derived over the years ranging from more approximate electronic structure methods to atomistic potentials, in which the electronic degrees of freedom are not explicitly taken into account. The aim of all these methods is to provide access to the potential energy surface (PES), which is defined as a high-dimensional function of the atomic positions yielding the potential energy. While computationally demanding electronic structure methods only permit the calculation of a few selected points on the PES, for atomistic potentials the PESs are usually defined by more or less sophisticated analytic functions of the atomic coordinates. Therefore, they can be evaluated several orders of magnitude faster and thus enable the calculation of very large numbers of configurations. In the present work the terms PES and atomistic potential will be used synonymously and the discussion will be restricted to the ground state PES. However, it should be noted that the methods outlined below can (and also have been) applied to excited state PESs. In general, constructing PESs for excited states is of similar complexity as the generation of ground state PESs, while obtaining the required information from electronic structure calculations can be significantly more challenging.

The existence and applicability of atomistic potentials depending only on the atomic positions without an explicit consideration of the electronic degrees of freedom can be derived from quantum mechanics (QM). Starting from the time-independent Schrödinger equation and assuming the validity of the Born–Oppenheimer approximation [9], the electronic Hamilton operator is fully defined by specifying the nuclear charges, i.e. the chemical elements, the atomic positions, and the total charge of the system, which is given by the number of electrons. Since, in turn, the sum of the expectation value of the electronic Hamilton operator and of the electrostatic repulsion between the nuclei yields the potential energy, the latter must be a function of the atomic configuration. This function is nothing else but the PES. If the PES were available in closed form, very efficient simulations could be carried out without solving the electronic structure problem again and again in each simulation step. Unfortunately, the topology of multidimensional PESs is extremely complicated for all but the most simple systems, since it is determined by the high complexity of the underlying quantum mechanical many-electron problem. Consequently, it is often a frustrating task to derive reliable analytic functional forms providing accurate potential energies that have a quality comparable to electronic structure methods.

In spite of these challenges, direct access to the PES would significantly facilitate the analysis and understanding of many processes, because the PES is of vital importance, e.g. for the determination of local and global minimum structures, but also for the identification of energy barriers and transition states, for the calculation of vibrational spectra, for the characterization of the structural and thermodynamic properties of molecules, liquids, and solids in computer simulations as well as, of course, for studying chemical reactions.

Generations of researchers have spent a lot of effort in devising and improving methods to construct atomistic potentials for all imaginable applications [10–16]. Without doubt, a lot of progress has been made, but still the construction of reliable potentials is far from trivial and often a lot of experience and chemical intuition are needed to obtain acceptable results. The quality and usefulness of atomistic potentials can be assessed by a number of criteria [17]:

The 'perfect potential' should:

(a) be as accurate as possible. Depending on the information that is used to construct the potential, there are two possible measures for the accuracy: the agreement with experiment or the agreement with reference data from electronic structure calculations.
(b) be transferable, i.e. it should work reliably for a wide range of atomic configurations and in particular for structures that have not been used for the construction of the potential.
(c) allow for systematic improvements in situations when it does not provide sufficiently accurate results. It should be easy to detect these situations without too much effort.
(d) be generally applicable to all types of systems like molecules, clusters, atomic and molecular liquids, ionic solids, semiconductors and bulk metals. This implies that the functional form of the potential should not contain any system-specific terms. Instead, it should be as generic as possible.
(e) be able to describe the making and breaking of bonds, i.e. it should be 'reactive'.
(f) take all relevant many-body interactions into account, which is important, e.g. for a reliable description of delocalized electrons in metals, or for considering electrostatic polarization in molecules. This can be achieved if the potential is sufficiently 'high-dimensional', i.e. its functional components should depend on many atomic coordinates.
(g) be fast to evaluate the potential energy of a large number of structures and/or large systems.
(h) have a well-defined functional form to permit the determination of analytic derivatives, which are needed to calculate, e.g. atomic forces, vibrational frequencies and, for periodic systems, the stress tensor.
(i) not require a significant amount of manual work and human intervention for its generation.
(j) not require an excessively large number of costly electronic structure calculations for the determination of its parameters.

The straightforward but computationally most demanding way to fulfill all these requirements would be the direct application of high-level electronic structure methods. Tremendous progress has been made in improving the efficiency of quantum chemical approaches, and a hierarchy ranging from very accurate post-Hartree–Fock methods like coupled cluster [18, 19] and configuration interaction [20, 21] to DFT [7, 8] is available. Consequently, the applicability of these techniques is expanding continuously, but there is no hope that in the foreseeable future even efficient methods like DFT

can be used in MD simulations of systems containing tens of thousands of atoms on a routine basis. Only if substantial approximations are introduced, which result in a notable loss of accuracy as in tight-binding [22, 23] and semi-empirical methods [24], can MD simulations of sizeable systems be carried out, but even then the computational costs remain significant. Therefore, many problems are still too demanding to be addressed directly by electronic structure methods.

On the other hand, the number of atomistic potentials available for studying very large systems is huge and probably hundreds or even thousands of new potentials or improvements of existing potentials are published each year for many different applications. Unfortunately, while being very efficient, no approach has yet been found that fully meets all the criteria listed above. Therefore, further progress in the development of atomistic potentials is urgently needed. This concerns both efficiency, e.g. for obtaining better simulation results by extending configurational sampling and for improving convergence with respect to system size, and also the quality of potentials, as there are still many chemical problems for which atomistic potentials are notoriously difficult to construct.

Important examples for challenging systems are:

- The self-assembly of organic molecules at metal surfaces, because very different types of interactions from covalent and metallic bonding to dispersion interactions are equally important. Closely related is also the field of heterogeneous catalysis, where additionally the ability to describe the making and breaking of bonds as well as a reliable representation of non-equilibrium configurations are of crucial importance.
- A wide range of inorganic materials exhibiting complicated and strongly varying atomic environments in complex crystal structures and, even worse, at defects like vacancies, interstitials, stacking faults, and grain boundaries. Further, structural phase transitions from one crystalline phase to another or even crystalline-to-amorphous phase transitions pose a significant challenge to any potential.
- The solid–liquid interface, where complex surface reconstructions have been observed and chemical reactions involving the dissociation and recombination of solvent molecules as well as the dissolution and deposition of surface atoms and other species are omnipresent.
- Nucleation events, ranging from crystallization in elemental melts, via the formation of ice in water, to more sophisticated biomineralization processes.
- The reliable description of unusual coordination geometries of ions, from solvation in highly concentrated aqueous solutions to the formation of metal–organic frameworks.

In the remaining part of this section, a simple classification scheme for atomistic potentials will be introduced, but it should be noted that also different types of categories could be used and that the classification is sometimes ambiguous. Further, we will focus on potentials not involving the direct solution of the electronic structure problem, but also this borderline is not always well defined. For instance, the bond order potentials developed by Pettifor, Drautz and coworkers represent a coarse-grained step that is based on the tight-binding method [25], and, on the other hand, approximate electronic structure methods like density-functional tight-binding (DFTB) [26–28] also contain some fitted terms.

Atomistic potentials have the common property that they establish a direct functional relation between the atomic positions and the potential energy. They comprise a wide range of approaches from simple classical force fields to very sophisticated and highly system-specific potentials. They will be classified here into two categories: 'physical' and 'mathematical' potentials. An alternative classification could also be based on the type of information that is used to construct the potentials, like 'empirical potentials' making use of experimental data that is sometimes augmented by theoretical results, and '*ab initio* potentials', which are exclusively based on data from electronic structure calculations.

For physical potentials, the functional form is typically derived by taking into account as much information about the system as possible. Often, more or less drastic approximations are made to reduce the complexity to a tractable level, while ensuring the essential physical properties are still properly described. This ensures that an overall reasonable performance in unexpected situations can be achieved even with a comparably small number of fitting parameters.

A very basic example of a physical potential is the Lennard–Jones (LJ) potential [29]. It is often used to describe van der Waals interactions in classical force fields [30–34]. Apart from the LJ potential, further typical components of force fields are two-body terms used to describe covalent bonds, three-body terms for angular contributions, and four-body terms for dihedral angles, as well as electrostatic interactions. In most cases, classical force fields are not able to describe the making and breaking of bonds and require predefined bonding patterns as well as the classification of atom types, e.g. according to particular functional groups.

Because of their very high efficiency and their ability to describe the geometry of common organic molecules with good accuracy, classical force fields are very popular in MD simulations of biochemical systems, where reactivity often plays a minor role. In combination with electronic structure methods focussing on the reactive parts, they are also often used in hybrid quantum mechanical/molecular mechanical (QM/MM) simulations [35]. In recent years, some of the limitations of classical force fields have been overcome by incorporating the ability to make and break bonds, e.g. in empirical valence bond potentials [36–38] and in the ReaxFF approach [39, 40], but here the overall functional form is still very similar to conventional force fields.

In materials science the requirements an atomistic potential should meet are very different. Here, an enormous variety of different chemical environments needs to be considered and often there is no way to clearly distinguish bonded from non-bonded atoms due to the broad spectrum of interatomic distances present in different crystal structures, large-scale defects and even amorphous systems. Therefore, the use of reactive potentials able to describe continuously changing atomic environments without the classification of atom types or predefined bonding patterns is mandatory.

An important and frequently used potential that was developed by Baskes and coworkers to describe metals is the embedded atom method (EAM) [41, 42] and its successor, the modified embedded atom method (MEAM) [43, 44]. In EAM, the system is considered as a composition of atoms, which are embedded into the electron densities arising from all their neighbors. The total energy is then given as a sum of the embedding energies of all atoms, which are determined from the electron densities of the atomic environments using an embedding function, and a pairwise repulsive potential. Usually, the electron densities are approximated as sums of free atom densities. In the MEAM extension, the accuracy of this approach was improved by including the angular dependence of the electron density.

Countless other types of physical potentials have been developed over the years to describe materials, like the Brenner potential [45, 46], the Tersoff potential [47, 48], and the Stillinger–Weber potential [49]. They rely on the concept of the bond order [50] to take into account the influence of the chemical environment on the bonding properties of atoms, but the identification of suitable functional forms and their parameterizations are generally very tedious tasks. The overall accuracy of all these potentials is limited by the constraints imposed by the functional form, and the quality of the description of physical properties depends on the specific parameters. Improvements for one property can often only be achieved by accepting a worse description of another [48]. Apart from these examples, many other types of physical potentials have been reported in the literature. They all have in common that the determination of the parameters involves a significant effort due to complex interdependencies, in particular for multicomponent systems. Often, the construction of these potentials has a large trial and error component.

To date, the vast majority of potentials belong to the class of physical potentials, but in recent years enormous progress has also been made in the development of purely mathematical approaches. Several powerful methods have emerged, which can provide extremely accurate energies and forces by employing highly flexible functional forms containing a large number of fitting parameters. Since the parameters of mathematical potentials are determined using a known data set obtained from electronic structure calculations and the shape of the PES is 'learned' from this training set, these techniques are also often described as 'machine learning'. Machine learning techniques are widely used for many purposes in mathematics and computer science [51–53], but their application to the representation of PESs is still relatively new and not yet widely distributed.

Many types of functions can be used to construct mathematical potentials, and they all have in common that they do not rely on any assumptions concerning the physical nature of the atomic interactions. Therefore, they can be called 'non-physical' (not to be confused with 'unphysical') to show that they are completely unbiased and do not favor one type of physical interaction over another. Functions proposed include polynomials, splines, Gaussians, sigmoid-like functions and many others.

The construction of interatomic potentials based on polynomials has been pioneered by Bowman and coworkers [54, 55]. Their aim has been to obtain very high accuracy and to incorporate the invariance of the PES with respect to a permutation of like atoms. This has been achieved in several steps: the construction of the potential starts with a complete set of interatomic distances, which are transformed to Morse coordinates to avoid a divergence of the potential for large atomic separations. Then, 'basis functions' consisting of monomials are constructed, which are symmetrized to ensure permutation invariance with respect to the interchange of atoms of the same chemical species. In the final step, the coefficients, typically a few thousand, of a truncated series of such polynomials are fitted using least-squares methods to a set of high-level electronic structure data. In some cases, e.g. for the interactions between three water molecules, damping functions can be used to improve the description of the system in the dissociation limit [56]. As a consequence of exploiting the permutation symmetry, it has been found that the number of *ab initio* calculations needed to construct the potential can be significantly reduced compared to a multiple calculation of equivalent geometries. The method has been developed for molecules and has been applied to a number of different systems with up to ten atoms [54], like CH_5^+ [57, 58], neutral and charged water clusters [56, 59, 60], the vinyl radical [61], and the CH_3CHO molecule [62].

An approach aiming to describe the PESs of solids and condensed systems is the Gaussian approximation potential (GAP) approach suggested by Bartók *et al* in 2010 [63]. Here, the total energy is constructed as a sum of environment-dependent atomic energies. The environments are defined by a cutoff function and the atomic densities inside these environments are projected onto the surface of a four-dimensional sphere. In a second step, the positions of the atoms on this sphere are described by an expansion using four-dimensional spherical harmonics. Then, Gaussians are placed on a set of points on the sphere corresponding to reference DFT calculations. The potential energy of unknown structures can then be obtained by interpolating the potential using a superposition of these Gaussians. In contrast to other PESs, in Gaussian processes the reference data are therefore not transferred to a set of fitting parameters, but the underlying data are directly used in the prediction of energies and forces of unknown configurations. This makes the method computationally more demanding when using large reference sets [64]. The method is extremely accurate, but the number of reported applications is still rather small. The first benchmark cases have been published for materials like carbon, silicon, germanium, iron and also the binary compound GaN [63]. The method has recently also been employed to fit one- and two-body corrections to the DFT PES of water using CCSD(T) reference calculations [64]. Apart from applications to construct potential energies, Gaussian processes, which are also called Kriging, have also been used by Popelier and coworkers to fit atom-centered electrostatic multipoles [65] with the aim of improving the accuracy of electrostatic interactions in classical force fields.

In the modified Shepard interpolation method of Collins and coworkers [66], the energy of an atomic configuration is constructed as a sum of weighted second order Taylor series expansions of inverted distances from known reference points.

While first developed for molecules in the gas phase [67], the method has been used extensively to study molecule-surface scattering [68, 69]. As with GAPs, an underlying training set is needed to predict the energies of new configurations, making the method more costly with larger reference data sets. Another challenge related to the use of Taylor series expansions is the need for second derivatives, which are difficult to obtain in reference electronic structure calculations. Many other mathematical potentials have been reported in the literature, like computationally rather demanding interpolating moving least-squares [70–73] and the combination of functions using genetic programming [74].

In this review, a mathematical potential based on artificial neural networks (NNs) [51] will be presented, which has been rapidly evolving in recent years and is applicable to molecular and condensed systems containing thousands of atoms. NNs, which were introduced more than 70 years ago, are a class of biology-inspired functions that have been applied successfully to a broad range of problems in many fields of science [52, 75]. While they have also found manifold use in chemistry and physics [76], to date the application of NNs to construct atomistic potentials is still not widely distributed, although this was already proposed two decades ago by Doren and coworkers [77]. As a consequence of some severe conceptual problems, the most important difficulty in using neural network potentials (NNPs) has been the restriction to very small systems with only a few degrees of freedom. For such small systems, however, electronic structure calculations are directly applicable, and many competitive techniques are readily available for the construction of highly accurate PESs if more CPU-time efficient potentials are required.

Here, an approach will be reviewed and discussed that overcomes the limitations of NNPs, which to date have prevented their wider use. Several NNPs for different types of systems, which have been published in recent years, demonstrate that the NNP method for high-dimensional systems has now become a practical tool for solving problems in chemistry and condensed matter physics involving a large number of atoms with complex bonding patterns.

2. Neural network potentials: state-of-the-art

2.1. A short historical overview

Artificial neurons were first introduced by McCulloch and Pitts in 1943 [78] as a simple mathematical tool for modeling signal processing in the nervous system. In analogy to neurons in biology, incoming signals are accumulated and, if a given threshold value is exceeded, the neuron itself sends a signal to its neighborhood. Otherwise, the neuron remains inactive. As a consequence of this step function-like behavior, artificial neurons are well suited to perform operations on binary numbers.

In 1958, Rosenblatt connected several artificial neurons organized in an input and an output layer to establish the first artificial NN, which has been called perceptron [79]. A problem of these early NNs was their inability to represent some logic functions, which was a severe drawback of the method

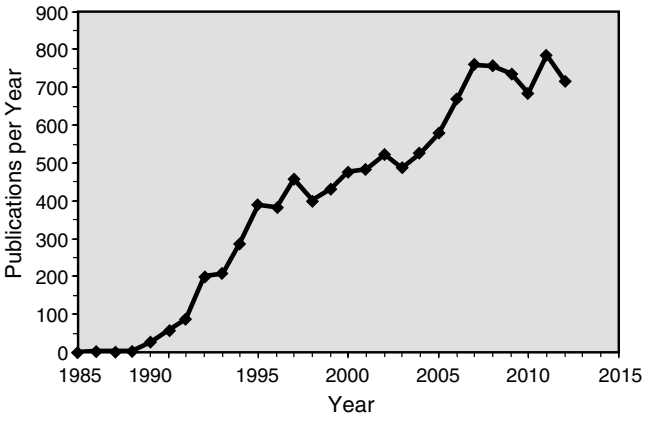

Figure 1. Number of publications per year in the field of chemistry making use of neural networks, extracted from the Web of Knowledge [85].

at that time since it was in competition with the rapidly expanding transistor-based computer technology. In 1969, Minsky and Papert [20] demonstrated that this limitation can be overcome by the introduction of a hidden layer of neurons in between the input and the output layer, which significantly extended the capabilities of NNs. Another challenge was the determination of the parameters of the NN. This problem was addressed successfully by Werbos in 1974 [80]. Further, in the same year, Little suggested replacing the step function by continuous non-linear functions [81]. Now, arbitrary NN output values could be obtained, which opened many new fields of applications beyond simple logic operations and classification problems.

In the 1980s and 1990s rapid progress was made in the development of NNs, and as an important research topic in mathematics and computer science they have found manifold use in almost all fields of science. Of high relevance for the present work is that it was proven independently by several groups that NNs are universal approximators [82, 83], i.e. that they are able to approximate unknown functions to, in principle, arbitrary accuracy if a set of function values is known:

> *Standard multilayer feedforward networks with as few as one hidden layer using arbitrary squashing functions are capable of approximating any Borel measurable function from one finite dimensional space to another to any desired accuracy, provided that sufficiently many hidden units are available. In this sense, multilayer feedforward networks are a class of universal approximators* [83].

Also in chemistry and physics NNs have found various applications [76, 84], which is demonstrated by the large number of results found in the Web of Knowledge [85] when searching for publications in the field of chemistry involving NNs (figure 1). Most of these papers employ NNs for pattern recognition and classification problems, e.g. for the analysis of spectra [86] or quantitative structure–activity relationship studies [87]. Although first suggested almost 20 years ago [77], NNs have not yet been used to construct many potential energy surfaces, and to date less than 100 papers have been published addressing the development or application of NNPs [17, 88, 89]. The main reasons for the small

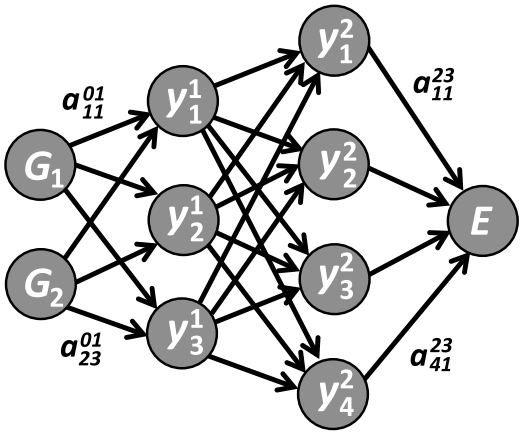

Figure 2. Schematic structure of a small feed-forward NN. Its analytic form is given by equation (2). For clarity the bias node and the bias weights are not shown.

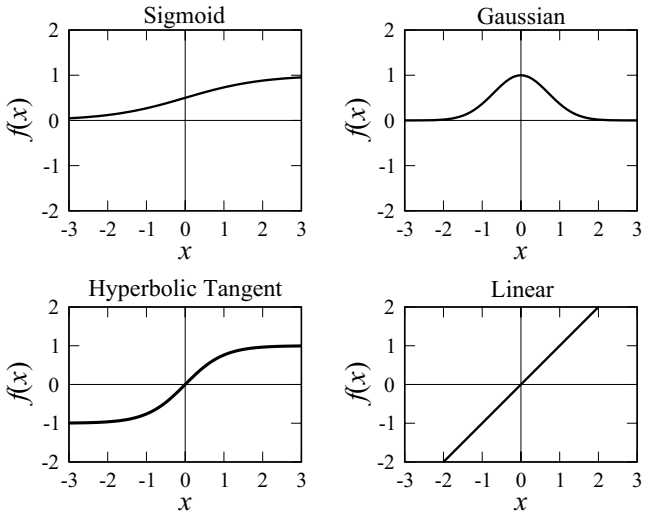

Figure 3. Typical activation functions used in feed-forward NNs.

number of studies are a number of conceptual problems, which to date have severely restricted the applicability of NNPs. In this review it will be shown how most of these problems can be overcome, making NNPs a valuable tool to represent the PESs of complex systems. Before these extensions are introduced section (3), some basic properties of NNs will be briefly summarized.

2.2. Feed-forward neural networks

A general definition of NNs was given by Kohonen in 1988 [90]: 'Artificial neural networks are massively parallel interconnected networks of simple (usually adaptive) elements and their hierarchical organizations, which are intended to interact with the objects of the real world in the same way as biological nervous systems do.'

Many different types of NNs have been proposed in the literature for various purposes [51]. For NNPs, feed-forward NNs are most frequently used. They consist of artificial neurons also called nodes, which are arranged in layers as shown in figure 2. The number of layers and the number of neurons per layer define the analytic form of the NN. The aim is to construct a functional relation between the input vector $\boldsymbol{G} = \{G_i\}$, whose components describe the atomic configuration and are supplied to the individual neurons of the input layer, and the output value, the energy E. In between the input and the output layer there are one or more hidden layers, which do not have a physical meaning. Instead, they define the functional form of the NN. The larger the numbers of layers and nodes per layer, the higher the flexibility and thus the ability of the NN to represent complicated functions. The arrows connecting the nodes in each layer to the nodes in the neighboring layers in figure 2 represent the fitting parameters of the NN and indicate the flow of information when the potential energy of a given structure is calculated. They are also called 'weights', because they are used as coefficients in linear combinations. The numerical value of a node i in layer j, y_i^j, is then calculated from the values of the nodes y_k^{j-1} in the previous layer $j-1$ according to

$$y_i^j = f_i^j\left(x_i^j\right) = f_i^j\left(b_i^j + \sum_{k=1}^{N_{j-1}} a_{k,i}^{j-1,j}\cdot y_k^{j-1}\right) \quad . \tag{1}$$

Here, $a_{k,i}^{j-1,j}$ is the weight connecting node k in layer $j-1$ with node i in layer j, and N_{j-1} is the number of nodes in the preceding layer. Apart from the input nodes each node in the NN is connected to a bias node, which provides a constant input value of one, by a bias weight b_i^j. It acts as an adjustable offset to shift the linear combination if needed.

After adding the bias weight, an activation function f_i^j, also called the transfer function or basis function, is applied to the shifted linear combination x_i^j. The purpose of the activation function, which is usually a non-linear function asymptotically converging to small numbers for very positive and very negative input values, is to allow the representation of arbitrary PESs. Some commonly used activation functions are shown in figure 3. In the output layer a linear function is applied to avoid any restriction on the range of NN output (energy) values.

The evaluation of the NN proceeds from the input layer via the hidden layers to the output layer. First, the values of the nodes in the first hidden layer are calculated from the input values $\{G_i\}$ using equation (1). Once they have been determined, they are used to evaluate the values of the nodes in the second hidden layer and so forth until finally the output node is reached. Overall, the NN corresponds to a nested function of rather simple terms represented by the activation functions. The full functional form of the example NN shown in figure 2 is then given by

$$\begin{aligned} E &= f_1^3\left(x_1^3\right) \\ &= f_1^3\left\{b_1^3 + \sum_{k=1}^{4} a_{k1}^{23}\cdot f_k^2\left[b_k^2 + \sum_{j=1}^{3} a_{jk}^{12}\cdot f_j^1\left(b_j^1 + \sum_{i=1}^{2} a_{ij}^{01}\cdot G_i\right)\right]\right\} \end{aligned} \tag{2}$$

The structure of the corresponding NN can also be specified using a short notation defining the number of nodes in each layer and the employed activation functions. If the hyperbolic

tangent is represented by t and the linear function by l, then the NN in figure 2 has a 2-3-4-1 *ttl* architecture.

The choice of a suitable NN architecture is very important: if there are too many neurons, the NN is too flexible giving rise to spurious features in the PES. If there are too few neurons, the NN is not able to resolve the shape of the PES correctly and important features may be missing, which results in large fitting errors. Although it has been suggested that the NN architecture can be determined on the fly together with the numerical values of the weight parameters [91], in practical applications it is more efficient to test a series of different NN architectures and to select the one providing the best representation of the PES.

Compared to physical potentials, the number of NN weight parameters N_w is typically very large and can be calculated according to

$$N_w = \sum_{k=1}^{M_{\mathrm{HL}}+1} (N_{k-1} \cdot N_k + N_k) \ . \tag{3}$$

This depends on the number of hidden layers M_{HL} and the number of neurons N_k in each layer k including the output layer. In total, NNs typically contain several thousand parameters. As a consequence, a large number of training points is required to determine the NN weights making the construction of NNPs rather costly. Further, due to their very general 'non-physical' functional form, NNPs have only limited extrapolation capabilities and are applicable with confidence only to the part of configuration space that has been used for training. As discussed below (section 4), fortunately it is straightforward to check if an NNP is reliable for a given set of structures, and it is easy to extend its range of validity if this is not the case.

NNPs offer a lot of advantages for the construction of atomistic potentials: they are able to represent PESs very accurately with results close to those of the underlying electronic structure method, while they can be calculated many orders of magnitude faster. They are continuous and differentiable and do not require any ad hoc approximations or manually constructed functional forms. Further, they are equally applicable to all types of bonded and non-bonded interactions, and, as analytic functions, analytic derivatives can be calculated, which are needed, e.g. for obtaining the atomic forces in MD simulations.

2.3. Definition of neural network potentials

A variety of NNPs, which employ one or even several feed-forward NNs to construct the total energy, have been published in the past two decades [17, 88, 92]. Still, surprisingly, no definition of NNPs has been proposed in the literature yet. In this work, an NNP is defined as an interatomic potential fulfilling the following three criteria:

- An NNP is an atomistic potential employing NNs to express a multidimensional function of the atomic coordinates yielding the potential energy.
- An NNP is constructed from a set of consistent energies (and sometimes forces) obtained using a specific reference electronic structure method.
- An NNP does not contain any physical approximations apart from those involved in the chosen reference electronic structure method.

The first criterion states that in contrast to most classical force fields, with NNPs a system is fully defined by the charges and the positions of the nuclei. No classification of atomic types, e.g. according to hybridization or functional groups, and no distinction between bonded and non-bonded interactions are necessary. Therefore, the information required for the application of NNPs is essentially the same as the input for electronic structure calculations. As a consequence NNPs are reactive, i.e. they are able to describe the making and breaking of bonds. The positions of the atoms can be provided in many different types of coordinates as long as some important conditions are fulfilled (section 3.3). Since NNPs have a well-defined functional form, analytic forces are easily accessible, which is an essential prerequisite for applications like geometry optimizations or MD simulations.

According to the second point, no experimental data should be used to construct an NNP. For any reference electronic structure method, there are necessarily some deviations between theoretically determined physical quantities, like equilibrium bond lengths, and their experimental counterparts. This is not only a consequence of the unavoidable uncertainty of experimental data but also of the numerical limitations of practical electronic structure calculations. If both experimental and theoretical data were used in the construction of an NNP, these data would not be consistent, giving rise to problems in the determination of the NN parameters. For the same reason, different levels of theory for the reference calculations should not be used together.

Criterion three implies that NNPs do not contain any system-specific terms, which could in principle be introduced to facilitate the description of the main features of the PES. Even if such terms have a sound physical basis, they should not be included in NNPs if they contain approximations restricting the accuracy or if they are not fully general. Examples of physical terms that may be useful in the construction of NNPs because they are exact and fully transferable are electrostatic interactions (section 3.2). Finally, the restriction of a given NNP to a single electronic structure method has the consequence that NNPs cannot be more accurate than the underlying reference method. Any deviation of the NNP from the reference PES, even if it provides results closer to experiment, is by definition considered as an 'error' of the NNP. The quality of an NNP can thus only be improved by choosing a higher-level reference electronic structure method or by using more training data if the inaccuracy is caused by an insufficient amount of data.

In summary, the primary goal of NNPs is to obtain highly accurate PESs, which provide potential energies that are as close as possible to a given reference electronic structure method. Efficiency plays only a secondary role. This is an important difference to many other types of potentials, which focus on the highest possible computational efficiency.

Table 1. List of NNPs for molecular systems published to date.

Year	Ref.	System	Reference method
1996	Tafeit *et al* [200]	Tetrahydrobiopterin	Hartree–Fock
1996	Brown *et al* [201]	$(HF)_2$	analytic PES
1996	Brown *et al* [201]	HF-HCl complex	Hartree–Fock
1997	No *et al* [202]	$(H_2O)_2$	MP2
1998	Gassner *et al* [124]	H_2O-Al^{3+}-H_2O	Hartree–Fock
1998	Prudente and Soares Neto [203]	HCl^+	Configuration interaction
1998	Prudente *et al* [204]	H_3^+	—
2002	Cho *et al* [205]	$(H_2O)_2$ in TIP4P	MP2
2003	Rocha Filho *et al* [206]	H_3^+	—
2004	Bittencourt *et al* [207]	OH	MRCI
2005	Raff *et al* [208]	vinyl bromide	MP4
2005	Raff *et al* [208]	Si_5 clusters	DFT (B3LYP)
2006	Agrawal *et al* [209]	SiO_2 molecule	DFT (B3LYP)
2006	Manzhos *et al* [94]	H_2O molecule	analytic PES
2006	Manzhos *et al* [93, 94]	HOOH	analytic PES
2006	Manzhos *et al* [94]	H_2CO	analytic PES
2006	Manzhos *et al* [93]	NOCl	analytic PES
2007	Houlding *et al* [110]	$(HF)_2$	DFT (B3LYP)
2008	Darley *et al* [111]	glycine	DFT (B3LYP)
2008	Darley *et al* [111]	N-methylacetamide	DFT (B3LYP)
2008	Malshe *et al* [210]	Si_5 clusters	DFT (B3LYP)
2008	Lee and Raff [211]	HONO	MP4
2009	Malshe *et al* [98, 212]	vinyl bromide	MP4
2009	Pukrittayakamee *et al* [213]	H+HBr	analytic PES
2009	Le *et al* [214]	HOOH	MP2
2009	Handley *et al* [112, 113]	water clusters	DFT (B3LYP)
2010	Le and Raff [215]	BeH + H_2	MP2
2010	Manzhos *et al* [216]	CO-$(pH_2)_n$	Coupled cluster
2011	Le *et al* [217]	O_3	MP4
2012	Nguyen and Le [218]	H_2O, ClOOCl	MP2
2013	Chen *et al* [219]	OH+CO	Coupled cluster
2013	Chen, Xu, and Zhang [220]	H_2 +OH	Coupled cluster
2013	Jiang and Guo [221]	H+H_2, Cl+H_2	analytic PES
2013	Li *et al* [120]	F+H_2O	MRCI
2013	Nguyen-Truong *et al* [222]	B_2S	DFT (B3LYP)

2.4. Conventional neural network potentials

In the past two decades NNPs have been constructed for many systems, which all have in common that they contain only a few degrees of freedom. These systems can be classified as small molecules (or groups of molecules) with up to about six atoms or as the interactions of small molecules with solid surfaces. In the latter, it is usually necessary to reduce the complexity of the system by fixing the atoms of the surface, which is a drastic approximation that needs to be validated for each system very carefully. A comprehensive list of the published NNPs and their applications is compiled in table 1 for molecular systems and in table 2 for molecule-surface scattering. More details of these NNPs as well as their scope and limitations can be found in some recent reviews [17, 88, 89, 92].

Most conventional NNPs have in common that they construct the potential energy employing just a single feed-forward NN, but some NNPs have also been constructed using a combination of several NNs. Here, in particular the work of Manzhos and Carrington needs to be mentioned. They have developed a very promising systematic approach using a set of optimized coordinates and a high-dimensional model representation [93–97]. The essential idea of this method is that multidimensional PESs are developed in analogy to a many-body expansion as a sum of lower-dimensional terms, each of which only depends on a subset of the coordinates that can be determined without manual intervention. This summation is then truncated at a predefined order. As the number of terms, which all correspond to individual feed-forward NNs, grows rapidly with the order of the expansion but also with system size, for computational reasons the method is only applicable to molecules containing about five or six atoms. For such systems, results of very high quality can be obtained. A similar approach, which is also based in spirit on a many-body expansion, has been developed and applied to vinyl bromide by Raff and coworkers [98]. A more detailed description and comparison of these two method can be found elsewhere [17].

3. High-dimensional neural network potentials

3.1. Limitations of conventional neural network potentials

Since the advent of the first NNPs, the restriction to low-dimensional systems has been a serious disadvantage of the method, and consequently only a small number of potentials have been reported to date. These studies demonstrate that NNPs are able to represent the PESs of small systems with very high accuracy. Still, apart from this proof-of-principle work, only a few ‘real’ chemical problems could be addressed, in most cases involving the reactive scattering of diatomic molecules at surfaces. Molecular systems, on the other hand, have mainly been used for investigating the fundamental capabilities of the approach and for methodical developments, while the number of atoms has been too small to answer questions

Table 2. List of NNPs for molecule–surface interactions published to date.

Year	Ref.	System	Reference method
1995	Blank *et al* [77]	CO @ Ni(1 1 1)	empirical PES
1995	Blank *et al* [77]	H_2 @ Si(1 0 0)-(2 × 1)	DFT (LDA)
2004	Lorenz *et al* [223]	H_2 @ K(2 × 2)/Pd(1 0 0)	DFT (PW91)
2005	Behler *et al* [123, 224, 225]	O_2 @ Al(1 1 1)	DFT (RPBE)
2006	Lorenz *et al* [226]	H_2 @ Pd(1 0 0)	empirical PES
2006	Lorenz *et al* [226]	H_2 @ (2 × 2)S/Pd(1 0 0)	empirical PES
2007	Ludwig and Vlachos [227]	H_2 @ Pt(1 1 1)	empirical PES
2007	Ludwig and Vlachos [227]	H_2 @ Pt(1 1 1)	DFT (PW91)
2008	Behler *et al* [225]	O_2 @ Al(1 1 1)	DFT (PBE)
2008	Latino *et al* [228]	ethanol @ Au(1 1 1)	DFT (B3LYP)
2008	Carbogno *et al* [229]	O_2 @ Al(1 1 1)	DFT (RPBE)
2009	Manzhos *et al* [97]	N_2O @ Cu(1 0 0)	DFT
2009	Carbogno *et al* [230]	O_2 @ Al(1 1 1)	DFT (RPBE)
2010	Latino *et al* [231]	ethanol @ Au(1 1 1)	DFT (B3LYP)
2010	Manzhos and Yamashita [232]	N_2O @ Cu(1 0 0)	DFT
2012	Goikoetxea *et al* [233]	O_2 @ Ag(1 1 1)	DFT (PBE)
2013	Liu *et al* [234]	HCl @ Au(1 1 1)	DFT (PW91)

that could not be addressed by other methods equally well. For most chemical problems a significant extension of the system size would be required to make NNPs a competitive approach in the field of atomistic simulations.

There are several conceptual problems that need to be solved to extend the applicability of NNPs to high-dimensional systems. First, the size of feed-forward NNs, i.e. the number of layers and nodes per layer, cannot be increased arbitrarily. Each new atom in the system introduces three additional degrees of freedom, which increases the number of nodes required in the input layer. Further, with a growing number of input nodes, also the number of nodes in the hidden layers needs to be adjusted to properly process the structural information. Necessarily, with increasing size, the computational performance of the NN evaluation decreases. Further, the number of weight parameters grows substantially with the size of the NN making the determination of the optimum set of weights more challenging. Finally, the rapidly increasing configuration space, which needs to be covered by the reference electronic structure calculations, does not allow for an arbitrary extension of the system size if its full complexity is described by a single NN.

A second problem for any conventional NNP consisting of a single NN is that it is only applicable to the system size that has been used for its construction, because once the numerical values of the weights have been determined, the number of NN input nodes cannot be changed. If an atom is added to the system, the NN weights connecting the input nodes representing its degrees of freedom for the first hidden layer are not available. If, on the other hand, an atom is removed, the numerical values of its input nodes are no longer defined. Of course, it is not acceptable to fit a separate NNP for each system size, because constructing a large set of potentials to study, e.g. different water clusters or metal particles with various numbers of atoms, is neither feasible nor desirable.

The most important challenge common to all NNPs is, however, the incorporation of the invariance of the potential energy of a system with respect to any transformation that does not change its structure. This involves the invariance of the energy of a molecule with respect to translation and rotation, but also the permutation symmetry regarding the interchange of chemically equivalent atoms, like the two hydrogen atoms in a free water molecule. Obtaining NNPs having these properties has been a severe challenge. The underlying problem is that the NN is just processing numbers describing the positions of the atoms in the system. If these numbers are not invariant with respect to rotation, translation or permutation, then the potential energy output of the NN is not invariant. A prominent example of an unsuitable set of coordinates are Cartesian coordinates, whose absolute values have no physical meaning since only relative atomic positions are important for the potential energy of a system. The main problem for obtaining an NNP with permutation symmetry upon exchange of like atoms is that the input coordinates of the NN form an ordered vector. Since different input coordinates, even if they refer to atoms of the same element, are connected to the NN by numerically different weight parameters, a permutation of any pair of atoms results in a change of the NN output. While this problem can be circumvented for small systems by using a well-defined order of atoms or by training the NNP using a reference set containing all equivalent representations of a molecule explicitly, for high-dimensional systems a rigorous solution must be found.

As a consequence of all these conceptual difficulties, it has been shown by several groups that NNPs are in principle a useful tool for constructing high-quality PESs, but applications aiming to solve real chemical problems, which cannot be addressed by other methods, have been very rare. In this review, we will first demonstrate that by solving these conceptual problems NNPs can be used to construct PESs of complex high-dimensional systems and, second, that these NNPs represent a valuable new method for performing large-scale simulations with significantly improved accuracy for many systems.

Before discussing the high-dimensional NNP method in detail, it should be noted that another high-dimensional potential employing NNs was suggested by Smith and coworkers in 1999 [99, 100]. In this approach the total energy is expressed by an NN of variable size using a set of input vectors obtained from a structural decomposition of the

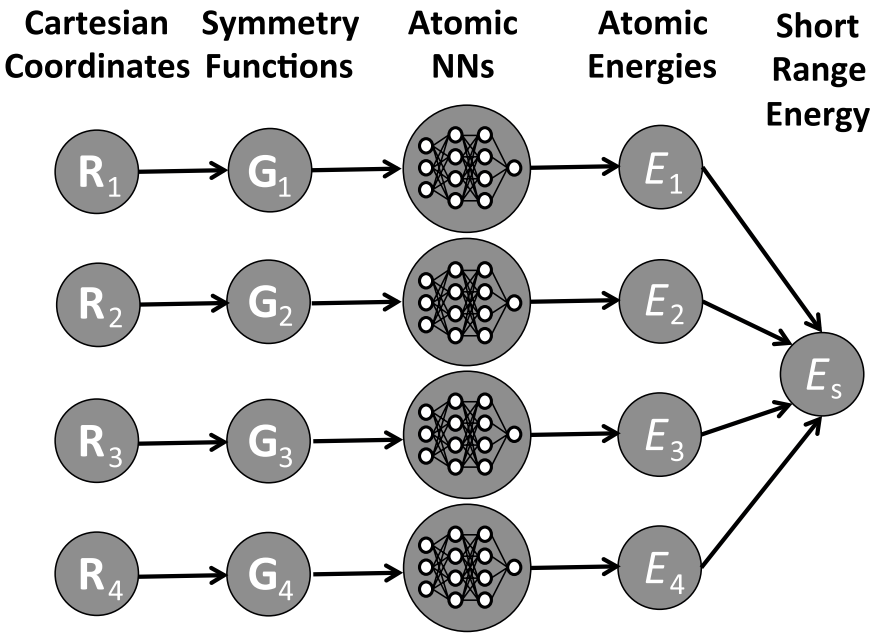

Figure 4. Example of a high-dimensional NNP for a four-atom system [103, 104]. Each line represents one atom i. Starting from the Cartesian coordinate vector $\boldsymbol{R}_i$, first a transformation to a symmetry function vector $\boldsymbol{G}_i$ is performed. This represents the input for the atomic NN yielding E_i. Finally, all atomic energies are added to obtain the (short-range) energy E_s.

system into a number of atomic chains of varying length. Since the potential does not use reference electronic structure calculations for training the weight parameters, it does not fulfill the formal criteria of an NNP given in section 2.3. Still, at that time it represented a very advanced approach, which, unfortunately, has only been applied to two benchmark studies for the binary hydrogen–carbon and carbon–nitrogen systems [100]. Surprisingly, after this early work the method was not used or extended for several years. Only in 2007 was the method taken up again and has been further developed into a genuine NNP for silicon, first based on tight-binding reference calculations [101], followed by an NNP employing DFT reference data in 2008 [102]. To date, no further applications of this method have been reported.

3.2. Structure of high-dimensional neural network potentials

The central idea of the high-dimensional NNP method reviewed here [103, 104] is the construction of the potential energy of a system using a set of atomic NNs instead of a single NN only. Each atomic NN, which corresponds to a standard feed-forward NN, provides as output the energy contribution E_i of atom i. The potential energy E_s is then given by the sum of all atomic energies,

$$E_s = \sum_{i=1}^{N_{\text{atom}}} E_i. \tag{4}$$

The atomic energies depend on the local chemical environments of the atoms, which are defined by a cutoff radius R_c. The positions of all atoms inside the cutoff sphere determine the atomic energy contribution, while atoms outside the cutoff do not contribute. The specific size of the cutoff radius needs to be determined in convergence tests until all relevant interactions are included, and we found that typically a value of 6–10 Å is sufficient. The dependence of the atomic energies on the local chemical environments corresponds to an effective reduction of the dimensionality to the energetically relevant interactions, while the total potential energy in equation (4) is still determined by all degrees of freedom of the system.

The input of the atomic NNs is given by a set of many-body symmetry functions, which will be described in more detail in section 3.3. For each atom they form a vector, which is a characteristic fingerprint of the atomic environment. The resulting high-dimensional NN scheme is shown schematically in figure 4 for a four-atom system. Each line represents one atom i starting from its Cartesian coordinate vector $\boldsymbol{R}_i$ on the left. Then a transformation of the coordinates to a symmetry function vector $\boldsymbol{G}_i$ is performed, which typically consists of 50–100 symmetry function values. Since these functions describe the atomic environment, they depend on the positions of all neighboring atoms within the cutoff radius. The $\boldsymbol{G}_i$ are then used as input for the corresponding atomic NNs yielding the E_i, which are added in the final step to obtain E_s.

It is important to note that for determining the weight parameters of the NN, it is not necessary to have access to individual atomic reference energies. Instead, the parameters of the atomic NNs are obtained using the total energy as the target quantity. This is important, because atomic energies are not observables and therefore they cannot be extracted from electronic structure calculations unambiguously, although some energy partitioning schemes have been proposed [105]. The optimization of the NN weights can then be carried out employing standard gradient-based optimization algorithms, which require the derivative of the total energy with respect to the weights of the atomic NNs.

There is only one type of atomic NN for each element, i.e. for a given chemical species the topologies of the atomic NNs

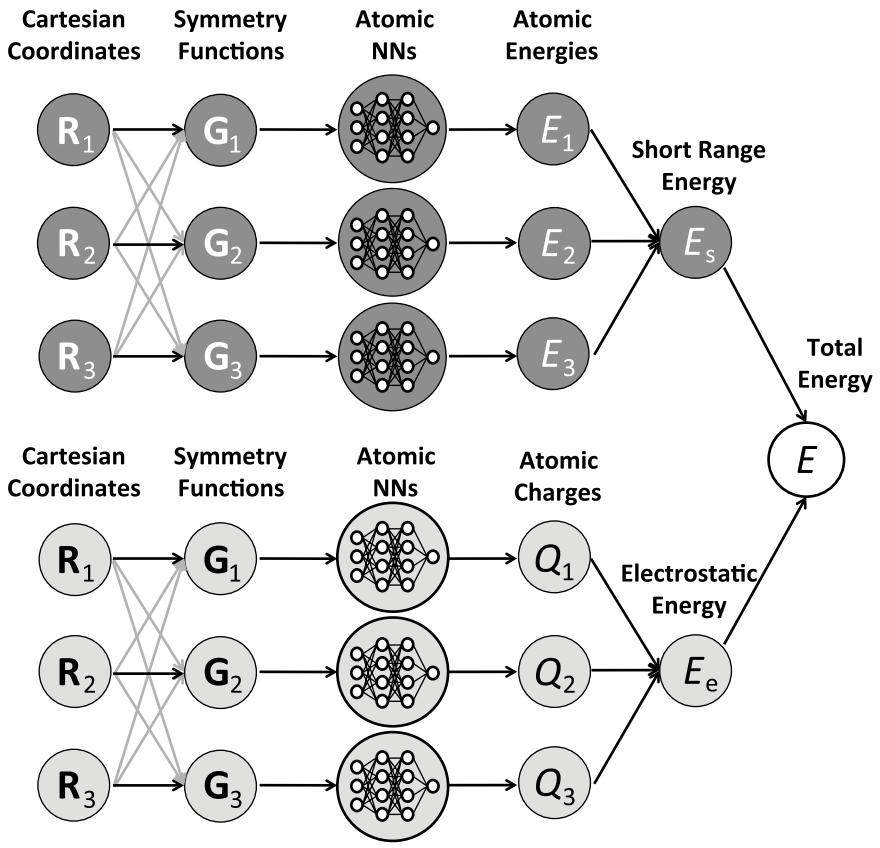

Figure 5. Schematic structure of a high-dimensional NNP for a three-atom system including electrostatics [106, 107]. The short-range part in the upper half of the figure corresponds to the scheme shown in figure 4. In the same way, a second set of atomic NNs is introduced to yield the environment-dependent atomic charges Q_i, which are then used to calculate the electrostatic energy.

and the weight parameters are identical. Therefore, if trained properly (section 4), the high-dimensional NNP method is applicable to arbitrary numbers of atoms by merely replicating the atomic NNs of the respective species as many times as needed. Further, as the potential energy is constructed as a sum of atomic energies, which is invariant with respect to the order of summation, the resulting energy is invariant with respect to permutations of the order of the atoms. Even for very large systems the structural complexity that needs to be processed by each individual atomic NN does not increase due to the employed cutoff, and therefore atomic NNs of very similar architecture, which are independent of the system, can be used. As one NN evaluation is needed per atom, once the NN weight parameters have been determined, high-dimensional NNPs can be used for very large systems and the computational costs scale linearly with system size. Further, since each atomic NN can be calculated independently, the method is also well suited for parallel implementations. Finally, the description of the atomic environments by many-body symmetry functions ensures that the atomic energies are invariant with respect to rotation and translation of the system (section 3.3). In summary, this method fulfills all requirements of high-dimensional NNPs discussed in the previous section.

There is only one approximation in this approach, which is the cutoff radius defining the range of the atomic interactions. While a very large cutoff can be chosen, in practical applications the performance of the method is significantly reduced if the cutoff is too large. Therefore, it is advantageous to take long-range interactions into account explicitly. As the cutoff is still notably larger than for many other potentials, the only relevant long-range interactions that may not be captured completely are electrostatic ones. In particular, for multicomponent systems with significant charge transfer between atoms of different elements, electrostatic interactions may be important. In order to include these interactions explicitly, the total energy expression has been generalized by employing equation (4) for the 'short-range' interactions E_s only. Further, the electrostatic energy contribution E_{elec} is calculated by an additional term [106, 107] resulting in the total energy expression

$$E_{tot} = E_s + E_{elec}. \tag{5}$$

In order to calculate the electrostatic energy the atomic charges need to be known. They are constructed by full analogy to the atomic energy contributions as environment-dependent charges $\{Q_i\}$, which are obtained from a second set of atomic NNs as shown in figure 5. Like in case of the short-range atomic energy contributions E_i, the chemical environments determining the atomic charges are defined by a cutoff radius and described by a set of many-body symmetry functions.

Employing these charges, the electrostatic energy contribution is then calculated by standard procedures according to Coulomb's law for non-periodic systems, or an Ewald summation [108] for periodic systems. Using the generalized high-dimensional NN method, the range of the electrostatic interactions is not truncated, while the atomic charges used

to calculate E_{elec} only depend on the local chemical environments. For short interatomic distances the electrostatic interactions can also be included in the short-range energies and forces, which can be used to introduce a screening of the electrostatic energy for close atomic encounters [107]. This screening has the advantage that an increased corrugation of the short-range energies can be avoided, which could arise by removing large electrostatic energies from total energies that are rather smooth.

There are several possibilities for training the atomic NNs providing the charges. While in principle the NN weights governing the charges could be determined simultaneously with the short-range NN weights, employing a single constraint that the smallest possible error of the resulting total energies should be obtained, this is a very complex coupled optimization problem. Therefore, it is advantageous to separate the training of the electrostatic NNs and the short-range NNs in the following way: first, atomic partial charges are determined in DFT calculations. There are many partitioning schemes available, and we usually use the Hirshfeld method [109], since Hirshfeld charges are not sensitive to the specific basis sets employed in the reference DFT calculations. Then the atomic NNs are trained to reproduce these charges as accurately as possible. In a second step, the NN atomic charges are used to calculate for each structure in the training set the electrostatic energy and forces, which are then removed from the DFT total energy and forces to obtain the short-range energy and force contributions. In the final step, these short-range components are then used to optimize the weight parameters of the short-range NNs. When the resulting NNP is applied to new structures, the electrostatic energy and the short-range energy can be calculated independently and are then combined to yield the total energy.

Several comments should be made concerning the extended NNP method including electrostatics. First, since the calculation of electrostatic interactions is physically exact and does not involve approximations reducing the accuracy, the formal definition of NNPs given in section 2.3 is still fulfilled. The only choice that is to some extent arbitrary is the selection of the Hirshfeld method to generate the reference charges. Since each charge partitioning method yields slightly different charges and thus also different electrostatic energies, this is in principle an approximation. However, the NN total energy is not sensitive to this choice at all, because the short-range energy is defined as the difference between the total energy and the electrostatic energy. Any error in the electrostatic energy will thus be compensated automatically by the short-range energy inside the cutoff radius. Only outside the cutoff radius does this error compensation not work, but the resulting errors are extremely small, and for large interatomic distances the differences between the charges obtained from different partitioning methods are usually quite small due to the negligible overlap of the electron densities.

Another important point to be considered is that for periodic systems overall charge neutrality must be ensured. Since the fitted NN charges have small remaining errors, it cannot be taken for granted that the sum of all atomic charges yields an exactly neutral system. In order to avoid complications in the Ewald summation, in practical applications of NNPs including electrostatics the NN charges are rescaled to yield neutral systems before they are used to determine the electrostatic energy and forces. The modification of the charges by this scaling step is usually about one order of magnitude smaller than the fitting error, which is typically only about 0.001 e. We further note that NNs have not only been applied to represent atomic charges, since it has been suggested by Popelier and coworkers that NNs could be employed to construct electrostatic multipoles to improve the description of electrostatic interactions in classical force fields [110–113]. In this approach, which by itself does not represent a self-contained NNP, the structure of the environment has been taken into account.

Finally, it should be mentioned that it is possible to improve the description of van der Waals interactions in high-dimensional NNPs in a straightforward way [114]. A correction of van der Waals interactions is not a requirement of the NNP approach itself as the short-range part is able to describe any type of atomic interaction as long as the cutoff radius is sufficiently large. Still, the quality of the description of van der Waals interactions can be low if DFT calculations are used for training the NNs. It has been known for a long time that current exchange-correlation functionals based on the generalized gradient approximation (GGA), which are still dominant in the literature, are not able to describe van der Waals interactions with sufficient accuracy. Consequently, in recent years, the development of correction schemes has been a very active field of research and a number of methods have been proposed [115–118]. Since the NN energies are numerically extremely close to the underlying DFT data, in particular the D3 method suggested by Grimme [119] can easily be combined with NNPs even after the construction of the NNP employing plain DFT-GGA data has been completed. For this purpose no modification of the NN weight parameters is required.

3.3. Symmetry functions for high-dimensional neural network potentials

3.3.1. Properties of symmetry functions. Apart from using a set of NNs to construct the individual atomic energy contributions and charges, the second crucial component of high-dimensional NNPs is a suitable set of many-body functions to describe the local chemical environments. The choice of coordinates is in general a very important aspect of the construction of any type of mathematical potential, and several functional forms have been proposed, depending on the specific method, to ensure the invariance of the potential energy with respect to rotation, translation and permutation, such as permutation invariant polynomials [60, 120], Coulomb matrices [121] and four-dimensional spherical harmonics [63, 122].

For NNPs, the NN input coordinates will be called ‘symmetry functions’ here, because they have the same numerical values for all energetically equivalent representations of a system. Historically, the term ‘symmetry function’ was introduced because these functions can be used to take the symmetry of ideal low-index single crystal surfaces into account [123]. These days the term symmetry function is used in a much broader context, referring not only to formal symmetry operations but to all operations leaving the *relative* atomic

configuration of the system unchanged. In general, suitable sets of symmetry functions need to fulfill the following criteria:

(a) They need to be continuous in value and slope.
(b) They must be invariant with respect to translation and rotation of the system.
(c) The vector of symmetry function values has to be invariant with respect to permutations in the order of chemically equivalent atoms in the atomic environments.
(d) The number of symmetry functions in the NN input vector must be the same irrespective of the number of atoms in the chemical environment.

The first point is a mandatory condition for constructing meaningful PESs, which must be continuous and differentiable in order to be applicable to MD simulations requiring the calculation of forces.

The second condition can be met by employing internal coordinates instead of Cartesian coordinates, because internal coordinates, such as interatomic distances, angles and dihedral angles, are invariant with respect to rotations and translations of the system. Indeed, internal coordinates have been frequently used for constructing NNPs of small molecular systems, but there are also problems arising from this choice. The number of internal coordinates grows rapidly with system size and if a full set of coordinates is used, they contain redundant information. If only a minimal set of internal coordinates is used, the selection of these coordinates is not well defined unless the atoms maintain a given order, which is not always easy to achieve. As a pragmatic solution, using a full distance matrix has been proposed for describing the structure, but this is only feasible for small systems due to the rapidly increasing size of the matrix with the number of atoms.

An even more severe problem with using internal coordinates concerns the permutation symmetry of the potential energy function with respect to the interchange of the positions of any two atoms of the same element. Even in very small systems like a single water molecule the exchange of the order of both hydrogen atoms will change the NN energy although chemically the system is still the same. The reason for this finding is that the coordinates in the input vector are ordered. Then, as all input nodes are connected to the NN by numerically different weight parameters, exchanging the order of both OH distances results in a different NN output. A problematic solution, which ensures only a numerical incorporation of the permutation symmetry, would be to train the NNP by using all chemically equivalent representations of a system, but this is computationally more demanding and does not guarantee an exact treatment of the symmetry. An ingenious way to take the permutation symmetry in small molecules into account was suggested in a seminal paper by Gassner *et al* [124]. It employs the three-body interactions in water molecules in the presence of an Al^{3+} ion as an illustrative example. In this work, a symmetrization scheme was introduced that is applicable to all kinds of molecules. Unfortunately, its complexity grows rapidly with system size, and therefore it is only applicable to systems containing up to about four chemically equivalent atoms. A similar approach has also been suggested for considering the symmetry in molecule-surface interactions by Behler, Lorenz and Reuter [123], but this method also is applicable only to small systems. In general, taking permutation symmetry into account could drastically reduce the number of training points by removing the need to include each structure many times in all possible atomic permutations [54]. This has also been recognized for other mathematical potentials like permutation invariant polynomials developed by Bowman and coworkers [60].

Finally, the independence of the number of symmetry functions from the number of atoms in the chemical environment is a specific requirement of high-dimensional NNPs, because in applications like MD simulations of large systems, atoms can enter and leave the spheres defined by the cutoff radius. This must not change the number of NN input nodes since otherwise the input vectors of the atomic NNs would not be well defined. Therefore, a given set of symmetry functions must be applicable without modification as the numbers of atoms vary in the chemical environments.

The derivation of suitable symmetry function coordinates fulfilling all the criteria listed above is one of the key steps towards the successful development of high-dimensional NNPs. Before specific functional forms of symmetry functions for high-dimensional NNPs are discussed, we note that the coordinate transformation to symmetry functions yielding the NN input vector is a crucial intermediate step of NNPs, which is much less important for conventional physical potentials. In the latter, the chosen functional form needs to take into account the equivalence of different possible representations and simultaneously has to yield the correct energy. For NNPs, these two steps are well separated: in a first step, the symmetry function values are determined. They ensure that all equivalent structural representations of a system are folded back into a unique set of values. Thus, in the second step the only purpose of the NN is to assign the energy to the input vector without having to consider any kind of symmetry in the system. This separation of the PES construction into two independent steps greatly facilitates the construction of reliable potentials. In many conventional physical potentials this separation is not so relevant, because only comparably low-dimensional terms are used, for which including the required invariances is not particularly challenging. An example are the simple additive two-, three- and four-body terms in classical force fields. For complex many-body potentials like NNPs, which include terms depending on hundreds of coordinates, fulfilling all symmetry requirements is significantly more difficult.

3.3.2. Atom-centered symmetry functions. The construction of the many-body symmetry functions starts with defining the cutoff function, which determines the local chemical environments of the atoms. Two different cutoff functions of the distance R_{ij} between the reference atom i and its neighbor j can be used [104]. The first possibility, which is very similar to the cutoff suggested by Tersoff [47], is to use the function

$$f_{c,1}(R_{ij}) = \begin{cases} 0.5. \left[\cos\left(\frac{\pi R_{ij}}{R_c}\right)+1\right] & \text{for } R_{ij} \leqslant R_c \\ 0 & \text{for } R_{ij} > R_c. \end{cases} \quad (6)$$

For $R_{ij} < R_c$, this corresponds to the monotonously decreasing part of a cosine function and its value and the value of its first derivative are zero at $R_{ij} = R_c$. Outside the cutoff radius its value and slope are zero.

An alternative cutoff function, for which in addition also the second derivative decays to zero at R_c, is given by

$$f_{c,2}\left(R_{ij}\right) = \begin{cases} \tanh^3\left[1-\frac{R_{ij}}{R_c}\right] & \text{for } R_{ij} \leqslant R_c \\ 0 & \text{for } R_{ij} > R_c. \end{cases} \quad (7)$$

While $f_{c,2}$ is in principle more appropriate for the calculation of forces, since by construction discontinuities of the forces are avoided when atoms enter or leave the cutoff spheres during MD simulations, in practical applications we found that the cutoff function $f_{c,1}$ is well suited if a sufficiently large cutoff radius is used [104].

In general, the cutoff radius is a convergence parameter that needs to be increased until all energetically relevant atomic interactions are included, and we found that cutoff radii of 6–10 Å are sufficient for obtaining high-quality potentials. The correct choice of the cutoff radius is very important, because any interaction between atoms separated by more than R_c not covered by the electrostatic term is treated as noise and gives rise to increased fitting errors. The cutoff function, which from now on will be specified by f_c to represent either of the two possible functions, is an essential part of all many-body symmetry functions.

The symmetry functions used to describe the atomic environments according to equation (4) are also called 'atom-centered symmetry functions' [104] to distinguish them from the pair symmetry functions introduced below [125]. There are two types of atom-centered symmetry functions: radial and angular functions, which describe the radial and angular distribution of the neighboring atoms, respectively. Both are high-order many-body functions simultaneously depending on all atomic positions inside the cutoff sphere. The most basic radial function G_i^1 describing the environment of an atom i is a sum of the plain cutoff functions with respect to each neighboring atom j,

$$G_i^1 = \sum_{j=1}^{N_{atom}} f_c\left(R_{ij}\right). \quad (8)$$

The summation is required to obtain a single function value independent of the number of neighboring atoms, which ensures the fixed dimensionality of the NN input vector. Its physical interpretation is a coordination number within the cutoff radius. In multicomponent systems there is one function for each element in the system, i.e. the distribution is resolved by chemical species. The spatial extension of G_i^1 is completely defined by R_c, and several functions with different cutoff radii are typically used to resolve the detailed radial distribution of neighboring atoms. Cutoff radii that are too small should not be used in order to avoid artifacts in the forces at $R_{ij} = R_c$ [104]. In turn, a lack of symmetry functions covering short atomic separations can result in a poor description of the region close to the reference atom. This problem can be solved by employing instead the radial symmetry function

$$G_i^2 = \sum_{j=1}^{N_{atom}} e^{-\eta\left(R_{ij}-R_s\right)^2} \cdot f_c\left(R_{ij}\right). \quad (9)$$

Here, the cutoff radius can be kept at a large value for all functions, while the radial resolution is now determined by the Gaussian exponent η. A Gaussian function is a better choice than using the interatomic distance itself, because it decreases for increasing atomic separations and thus naturally reflects the decaying atomic interactions with growing distance. Again, the sum ensures that just a single number is obtained, and the radial resolution can now be controlled by using a set of functions with different Gaussian exponents. Functions of type G_i^2 do not introduce any artifacts in the forces if sufficiently large cutoff radii are used, which now even allows the region close to the reference atom to be covered [104]. Consequently they are generally superior to functions of type G_i^1. The parameter R_s can be used to improve the description of specific interatomic distances. While for $R_s = 0$ the Gaussians are centered at the reference atoms, for $R_s \neq 0$ the Gaussians form spherical shells of width given by η.

While a set of these functions can be used to describe the radial distribution of the neighboring atoms, it is not possible to distinguish different angular distributions in the atomic environments using only these functions. Therefore, in addition atom-centered angular symmetry functions are introduced for an accurate description of the chemical environments. There are two types of angular functions both depending on the angle $\theta_{ijk} = \frac{\mathbf{R_{ij}} \cdot \mathbf{R_{ik}}}{R_{ij} R_{ik}}$ centered at atom i, with $\mathbf{R_{ij}} = \mathbf{R_i} - \mathbf{R_j}$, and j and k being two neighboring atoms inside the cutoff sphere. They are

$$G_i^4 = 2^{1-\zeta} \sum_{j \neq i} \sum_{k \neq i,j} \left[\left(1 + \lambda \cdot \cos\theta_{ijk}\right)^\zeta \times e^{-\eta\left(R_{ij}^2 + R_{ik}^2 + R_{jk}^2\right)} \cdot f_c\left(R_{ij}\right) \cdot f_c\left(R_{ik}\right) \cdot f_c\left(R_{jk}\right) \right] \quad (10)$$

and

$$G_i^5 = 2^{1-\zeta} \sum_{j \neq i} \sum_{k \neq i,j} \left[\left(1 + \lambda \cdot \cos\theta_{ijk}\right)^\zeta \cdot e^{-\eta\left(R_{ij}^2 + R_{ik}^2\right)} \cdot f_c\left(R_{ij}\right) \cdot f_c\left(R_{ik}\right) \right]. \quad (11)$$

Instead of using the angle θ_{ijk} directly, its cosine is used to take the periodicity of the potential with respect to the angle into account. Parameter λ, which can have the values +1 and −1, determines whether the maxima of the cosine terms are located at $\theta_{ijk} = 0°$ or $\theta_{ijk} = 180°$. As with the radial functions, the cosine values of all atomic triples are added, yielding a single symmetry function value independent of the actual number of neighbors. The angular resolution can be controlled by the exponent ζ. Scanning the angular distribution at various distances from the reference atom is possible with the correct choice of the Gaussian exponent η. The main difference between the angular functions G^4 and G^5 is the absence of R_{jk}, the distance between neighboring atoms j and k, in function G^5. Consequently, for G^4 the angles are only considered if all three interatomic distances, R_{ij}, R_{ik} and R_{jk} are smaller than R_c, while for function G^5 the R_{jk} can have arbitrary values. A more detailed discussion of the properties of these symmetry functions and some plots can be found elsewhere [104].

The atom-centered symmetry functions presented here are not just used to construct atomic energy contributions in high-dimensional NNPs. Their ability to distinguish different atomic environments was recently employed by Geiger and Dellago to identify various polymorphs of ice [126]. In this work it was shown that atom-centered symmetry functions are superior to other commonly employed descriptors like Steinhardt bond order parameters [127].

3.3.3. Pair symmetry functions. Apart from constructing the total energy as a sum of atomic energy contributions according to equation (4), there is an equivalent expansion of the energy of a many-atom system in terms of pair energies E_{ij} [47],

$$E = \sum_i E_i = \sum_i \sum_{j \neq i} E_{ij}. \tag{12}$$

Following this alternative approach, we have also developed a set of 'pair symmetry functions', which are used to describe the chemical environments of atom pairs and can be used to construct the energy of a molecule or solid as a sum of environment-dependent pair energies [125]. In this approach, the atom pairs are defined as any couple of atoms separated by a distance shorter than the cutoff radius, and the environment of each pair is defined as the region covered by the two cutoff spheres centered at each of the atoms forming the pair. The same cutoff functions (see equations (6) and (7)) as for the atom-based NNPs can be used.

Before we start discussing the pair symmetry functions describing the chemical environments of the pairs, we note that this approach reduces to NN pair potentials, if the chemical environments are not considered. The most basic symmetry function that can be used to construct such an NN pair potential is the plain cutoff function,

$$G_{ij}^1 = f_c\left(R_{ij}\right). \tag{13}$$

In order to avoid discontinuities in the derivatives for small cutoff radii, it is advantageous to use a modified function consisting of a product of a cutoff function employing a large cutoff radius and a Gaussian to modify the spatial extension instead,

$$G_{ij}^2 = f_c\left(R_{ij}\right) \cdot \mathrm{e}^{-\eta R_{ij}^2} \tag{14}$$

Also this pair symmetry function can only be used to construct NN pair potentials as the chemical environment is still completely neglected.

To include the chemical environment explicitly, in analogy to the expansion of the total energy as a sum of atomic energies, radial and angular pair symmetry functions can be introduced. A novel aspect of pair symmetry functions is that for homonuclear pairs the permutation symmetry of the function value with respect to an interchange of both atomic positions defining the pair must be enforced. This can be achieved, for instance, by using the radial pair symmetry function

$$G_{ij}^3 = f_c\left(R_{ij}\right) \cdot \left[\sum_k f_c\left(R_{ik}\right) + \sum_k f_c\left(R_{jk}\right) \right], \tag{15}$$

which is the product of a cutoff function of the interatomic distance in the pair and the sum of two accumulated cutoff functions of the distances between any atom k in the environment and both atoms forming the pair. As for equation (14), a smoother decay of the symmetry function derivatives at the cutoff radius can be obtained by multiplying the cutoff functions by Gaussians and using large cutoff radii,

$$G_{ij}^4 = f_c\left(R_{ij}\right) \cdot \mathrm{e}^{-\eta \cdot R_{ij}^2} \left[\sum_k f_c\left(R_{ik}\right) \cdot \mathrm{e}^{-\eta \cdot R_{ik}^2} + \sum_k f_c\left(R_{jk}\right) \cdot \mathrm{e}^{-\eta \cdot R_{jk}^2} \right]. \tag{16}$$

An angular pair symmetry function can be introduced as

$$G_{ij}^5 = f_c\left(R_{ij}\right) \cdot \mathrm{e}^{-\eta \cdot R_{ij}^2} \times 2^{1-\zeta} \sum_{\theta_{kij}} \left[\left(1 + \lambda \cdot \cos\theta_{kij}\right)^{\zeta} \cdot \mathrm{e}^{-\eta \cdot \left(R_{ik}^2 + R_{jk}^2\right)} \cdot f_c\left(R_{ik}\right) \cdot f_c\left(R_{jk}\right) \right], \tag{17}$$

where we have defined θ_{kij} as the angle centered at the neighboring atom k for symmetry reasons. A more detailed discussion of the properties of the pair symmetry functions and a comparison of the performance of pair-based and atom-based high-dimensional NNPs for several systems can be found elsewhere [125]. In essence, we have found that the quality of NNPs based on atom pairs is at least comparable to the quality of NNPs using atom-centered symmetry functions, while, as expected, the computational efficiency is lower due to the larger number of pairs.

3.3.4. Constructing symmetry functions. Having introduced the functional forms of the symmetry functions, we now need to find a way to determine the specific parameters of the symmetry functions, which define their spatial shape. The most important parameter is the cutoff radius R_c. Here, a value that is too small will result in a loss of accuracy, because interactions beyond the cutoff radius will be treated as noise unless they can be described by the electrostatic term. Therefore, convergence tests need to be carried out to ensure that all relevant interactions are included. On the other hand, the cutoff should not be too large, because the configuration space spanned by the volume of the cutoff spheres needs to be described by the symmetry functions as precisely as possible, which becomes more challenging with larger cutoff radii.

The determination of the remaining parameters, η, R_s, ζ and λ, is currently more empirical, but here are some guidelines for how appropriate sets of symmetry functions can be constructed:

- The symmetry function values should be sufficiently different to avoid redundant information. This can be checked automatically for specific training sets by investigating the correlation between the symmetry function values. If the correlation is too high for any two symmetry functions, then one of these functions should be discarded.
- The symmetry functions need to clearly distinguish different chemical environments. If this is not possible, then different atomic environments may have very similar symmetry function vectors even though the target energies and forces to be represented by the NN are substantially different. This training with contradictory information results in poor quality potentials. A possible way to identify inadequate symmetry function sets is to compare pairwise the atomic forces and symmetry function vectors

for all atoms in the training set. If the symmetry function vectors are very similar while the forces are notably different, the symmetry function set is inadequate for distinguishing the structures [104]. This can be checked wholly automatically.There are many other requirements that should be fulfilled by the symmetry functions. For instance, for numerical reasons the range of values should be sufficiently large for any symmetry function to avoid numerical instabilities. Further, the relative importance of the symmetry functions can be balanced by normalizing the range of values of all symmetry functions.

In general, we found that sets of 50–100 symmetry functions are able to provide excellent structural fingerprints of the atomic environments resulting in typical total energy errors of only a few meV per atom. In the various systems we have studied so far we have found that the quality of the obtained NNPs is, surprisingly, not very sensitive to changes in the symmetry function sets and that in turn a given set of symmetry functions is applicable to very different systems like semiconductors, metals and oxides. Still, it would be desirable to develop a computational scheme to derive the optimum set of symmetry functions for arbitrary systems wholly automatically, and this work is currently in progress.

3.3.5. Energy gradients. As NNPs have well-defined functional forms, analytic energy gradients are readily available. They are required, e.g. for the determination of the atomic forces in applications like structural optimizations and MD simulations.

The calculation of the atomic force F_α with respect to the Cartesian coordinate α of some arbitrary atom in the system requires the derivatives of the short-range energy and of the electrostatic energy,

$$F_\alpha = -\frac{\partial E_\mathrm{s}}{\partial \alpha} - \frac{\partial E_\mathrm{elec}}{\partial \alpha}. \tag{18}$$

The short-range component of the force is then given by

$$\begin{aligned} F_{\alpha,\mathrm{s}} &= -\frac{\partial E_\mathrm{s}}{\partial \alpha} = -\sum_{j=1}^{N_\mathrm{atom}} \frac{\partial E_j}{\partial \alpha} \\ &= -\sum_{j=1}^{N_\mathrm{atom}} \sum_{\mu=1}^{N_{\mathrm{sym},j}} \frac{\partial E_j}{\partial G_{j\mu}} \cdot \frac{\partial G_{j\mu}}{\partial \alpha}, \end{aligned} \tag{19}$$

taking into account the transformation of the Cartesian coordinates of the atoms to the symmetry functions. Here, $N_{\mathrm{sym},j}$ is the number of symmetry functions describing the environment of atom j. The first term in the double sum of equation (19), i.e. the dependence of the atomic energy on the symmetry functions, is then given by the architecture of the atomic NNs, while the second term is defined by the functional forms of the symmetry functions.

For the derivative of the electrostatic energy, it is important to remember that the atomic charges are environment dependent, which gives rise to additional derivatives compared to conventional classical force fields employing fixed atomic charges. For non-periodic systems, the electrostatic force component is given by

$$\begin{aligned} F_{\alpha,\mathrm{elec}} &= -\frac{\partial}{\partial \alpha} \frac{1}{2} \sum_{i=1}^{N_\mathrm{atom}} \sum_{j=1, j\neq \mathrm{i}}^{N_\mathrm{atom}} \frac{Q_i Q_j}{R_{ij}} \\ &= -\sum_{i=1}^{N_\mathrm{atom}} \sum_{j=1, j\neq i}^{N_\mathrm{atom}} \frac{1}{2R_{ij}^2} \left[\frac{\partial Q_i}{\partial \alpha} Q_j R_{ij} + Q_i \frac{\partial Q_j}{\partial \alpha} R_{ij} - Q_i Q_j \frac{\partial R_{ij}}{\partial \alpha} \right] \end{aligned} \tag{20}$$

After some rearrangements, regrouping of indices and considering the transformation of the Cartesian coordinates to symmetry functions we finally obtain

$$F_{\alpha,\mathrm{elec}} = \sum_{j=1}^{N_\mathrm{atom}} \sum_{i=1, i\neq j}^{N_\mathrm{atom}} \frac{Q_i}{R_{ij}} \cdot \left[\frac{1}{2} \frac{Q_j}{R_{ij}} \frac{\partial R_{ij}}{\partial \alpha} - \sum_{k=1}^{N_{\mathrm{sym},j}} \frac{\partial Q_j}{\partial G_{jk}} \frac{\partial G_{jk}}{\partial \alpha} \right]. \tag{21}$$

For periodic systems, the corresponding equations are more complicated due to the employed Ewald summation, but the derivation is essentially the same.

In a similar way, other physical quantities depending on energy gradients can be calculated, like the stress tensor [104], which is needed for the determination of the static pressure in condensed systems, for MD simulations employing the NPT ensemble, and in metadynamics simulations of pressure-induced structural phase transitions [128].

4. Training neural network potentials and quality control

The most important part of constructing NNPs is the determination of a set of weight parameters that will provide accurate energies and forces for a wide range of atomic configurations. Obtaining a high transferability is the major goal here. Only if an NNP is able to provide reliable energies and forces for structures not included in the training set, will it be a useful tool for atomistic simulations of chemical processes. To reach this goal it is important but not sufficient to find weights that represent the training energies, forces and charges well. We also need to establish measures to assess the reliability of a prediction without performing an electronic structure calculation to check the potential, which would be unfeasible for a large number of structures.

The weight parameters are determined in an 'online learning' process, i.e. they are adjusted iteratively to reproduce a known data set of energies, forces and charges obtained from reference electronic structure calculations. The first goal is to minimize the root mean squared error (RMSE), which is defined, e.g. for the energies by

$$\mathrm{RMSE} = \sqrt{\frac{1}{N_\mathrm{struct}} \sum_{i=1}^{N_\mathrm{struct}} \left(E_{i,\mathrm{ref}} - E_{i,\mathrm{NN}} \right)^2}. \tag{22}$$

Similar expressions are used for the forces and the charges, and it should be noted that the error minimizations of the short-range energies and forces are coupled, because they depend on the same set of weights.

Many different optimization algorithms can be employed to determine the numerical values of the weight parameters [129]. Usually, gradient-based optimization algorithms

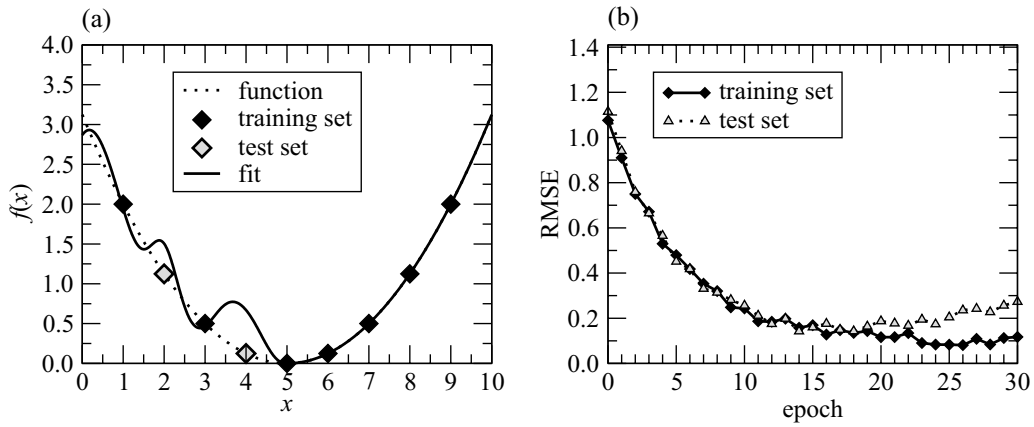

Figure 6. In overfitting (*a*), only the training points are well represented and therefore close to the target function $f(x)$, while the points in the test set have a significantly larger error. In the early stopping method, the errors for the training and the test sets are monitored during the fit. (*b*) The optimum fit. The best fit corresponds to the set of weights minimizing the error for the test set, since this fit has the best transferability to structures not included in the training set. An increasing error for the test set indicates the onset of overfitting.

are used. They require the derivatives of the NN error with respect to the individual weights, which reduces to the calculation of derivatives of the NN short-range energies, short-range forces and charges, since the corresponding reference values are independent of the NN weights. In the context of NNs, the backpropagation algorithm is the most established method [130], but the adaptive global extended Kalman filter [131–133] and the Levenberg–Marquardt algorithm [134] have been used frequently. Other techniques that have been proposed are swarm searches [129], simulated annealing [129], genetic algorithms [129, 135] and combinations of these methods. Unfortunately, the optimization of the weight parameters is extremely challenging due to the large number of weights, and there is no hope of finding the global minimum. Still, in most cases it is possible to find sufficiently accurate local minima in the weight parameter space, which will provide reliable potentials.

While the quality of an NNP certainly depends on the magnitude of the RMSEs of the energies, forces and charges in the training set, even more important is the reliability of the NNP for configurations not included in this set. A basic procedure that is almost always used to estimate the accuracy of NNPs is the 'early stopping' method. Here, a part of the known reference structure is not used to optimize the NN weights, but it is employed as an independent test or validation set. During the iterative optimization of the weight parameters, the RMSEs of the training and the test sets are monitored, and the optimum fit can be identified in the following way (figure 6(*b*)): in the early stage of the fitting process the errors for both the training and the test sets decrease, as the NNP learns the overall features of the PES. Then, while the error for the training set gets smaller and smaller, the error for the test set typically reaches a minimum and starts to increase again. This is the onset of overfitting, which is defined as an improved description of structures in the training set at the cost of a worse description of structures in between (figure 6(*a*)). Since the NN does not have any information about the test points located in between the training points, all effort is put into the improvement of the training points only, and the worsening description of the structures in the test set is not visible in the RMSE of the training set. On the other hand, a reliable description of arbitrary atomic configurations is crucial for a successful application of an NNP. Therefore, the potential with the best overall description of the PES corresponds to the set of weights that minimizes the error of the test set. In a good NNP, the training and the test sets have very similar errors.

Still, the early stopping method is not sufficient to ensure that an NNP is always reliable, because any part of the configuration space that is not well represented in the reference electronic structure calculations will not be present either in the training set or in the test set. These 'holes' in the configuration space will thus remain undetected. Consequently, it may happen that the NN predicts energies and forces with spectacularly large errors for structures very different from the training structures. This is an immediate consequence of the 'non-physical', i.e. completely unbiased, functional form of the NN. Fortunately, this fundamental drawback of NNPs can be turned into a unique advantage and it can be used in a very elegant way to detect the holes in the reference set, to add missing training structures and to obtain converged NNPs.

In this procedure, initially several NNPs are constructed using the same reference set. They should have different functional forms, which can be enforced, e.g. by selecting different NN architectures. Then, NNPs with comparable errors are chosen and one of them is used to generate a large number of structures, for instance by extended MD or MC simulations. Afterwards, the energies and forces of these structures are recalculated by the other available NNPs and the energies and forces are compared to the respective values of the first NNP. The procedure is shown schematically in figure 7. If, for a given structure, the energy and the forces predicted by all the NNPs are very similar, then the structure is very likely close to a structure in the training set and the NNPs are reliable. If, on the other hand, all NNPs predict very different energies and forces, then in this part of the configuration space the NN has too much flexibility, because the set of training structures is too sparse. Such structures should then be added to the training set to improve the NNPs. This procedure, the generation of many structures by NNP-based simulations and the identification of structures missing in the training set, is

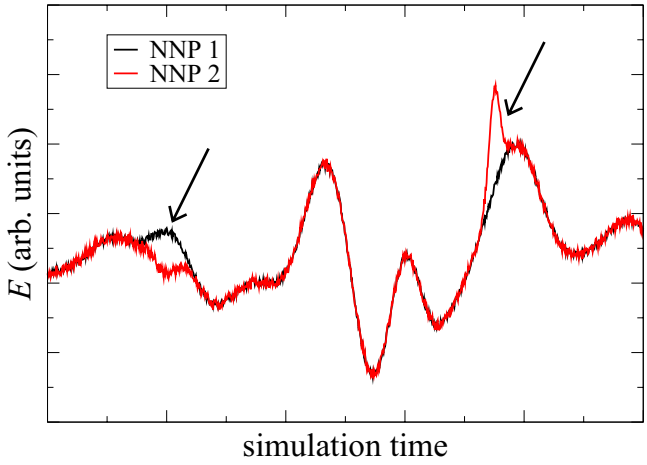

Figure 7. Validation of NNPs using MD simulations: first two or more NNPs are constructed using the same training set. Then NNP 1 is used to generate a large number of configurations by MD. The energies of these configurations are then recalculated by NNP 2. If the predictions are similar, the NNPs are reliable. If the NNPs predict very different energies, as in the two regions indicated by the arrows, then these structures should be added to the training set to improve the potentials.

repeated iteratively until the training set is sufficiently dense in all relevant parts of the configuration space.

This simple but very efficient technique has several advantages: First, it is not necessary to determine the relevant parts of configuration space beforehand, which is very difficult in high-dimensional systems where it is not possible to generate training structures on a regular multidimensional grid of points. Instead, the structures are generated under simulation conditions, i.e. they are relevant for the intended applications of the NNPs. Second, it is possible to identify important structures without carrying out costly electronic structure calculations for all structures on a trial and error basis. Instead, electronic structure calculations are needed only for those structures that have been proven to be missing in the training set.

The final comment to be made concerns the extrapolation capabilities of NNPs for structures outside the part of configuration space spanned by the training structures. For such structures the transferability is very limited, as for all mathematical potentials. For such extrapolation, NNPs will usually fail and the predicted energies and forces will have large errors. While in principle the same strategy described above could be used by employing several NNPs to check for extrapolation problems, there is a much simpler way to identify extrapolation. Extrapolation can easily be detected by an analysis of the symmetry function vector even before the energy and forces are calculated. For this purpose, for each symmetry function the minimum and maximum values are determined from the data in the training set. Then, whenever during an NNP-based simulation the energy and forces for a structure are requested, its symmetry function values are compared to these boundaries. If any symmetry function value is outside this range, an error message is issued and the simulation can be stopped. Like in the iterative improvement of the training set described above, these extrapolation events can be used to extend the structural range of validity of the NNP systematically by including these structures in the training set.

5. Applications of high-dimensional neural network potentials

In recent years, the high-dimensional NNP method has been applied successfully to the construction of very accurate potentials for a number of different systems using DFT as the reference method. The first application was the investigation of pressure-induced phase transitions in silicon [103, 136, 137]. Silicon has a very rich phase diagram [138] and has thus become an important benchmark system for the development of interatomic potentials in materials science [43, 45, 47, 49, 139–144]. Based on a training set of about 20 000 energies, a potential was derived that gave a very accurate description of all investigated crystal structures of silicon and a wide range of amorphous configurations. The remaining total energy errors were as low as about 5–6 meV/atom, which is the typical accuracy that can be achieved by NNPs. Employing this NNP, the full high-pressure phase diagram of silicon was obtained and it had excellent agreement with experiment and DFT [136, 137]. A series of metadynamics simulations [128, 145] at increasing pressures were used, which required only about 1% of the computer time that would be needed to carry out the simulations directly by DFT. The largest part of this computer time was spent on constructing the training set and fitting the NN parameters, while the computational costs for carrying out the actual simulations were negligible.

In another application it was demonstrated that NNPs can describe 'real surfaces' of metals, which often exhibit a wide range of defects, such as adatoms, vacancies, steps and kinks, using copper as an example system [146]. Since it is not possible to validate the NNP energies for structures containing many thousand atoms, which are beyond reach for reference electronic structure calculations, instead the atomic forces were used as local probes of the PES. For validation, DFT calculations can then be carried out for clusters centered at a number of representative atoms. If these clusters are sufficiently large, which has been tested in convergence tests, the forces acting on the central atoms are very close to the relevant forces in the full system. By performing this test for numerous atoms at various defects, it was shown that high-dimensional NNPs can provide reliable PESs for very large metal surface models [146], as well as for a number of different metallic bulk phases. Very similar tests have also been performed for ZnO as a typical metal oxide [106] with very similar results. In this case, the generalized high-dimensional NNP method including electrostatics was explicitly used for the first time.

These studies of copper and zinc oxide were motivated by the industrial application of mixtures of copper and ZnO particles as catalysts for methanol synthesis from synthesis gas. Due to the high commercial relevance of this process, but also because of its prototypical character for the role of oxide-supported metal clusters in heterogeneous catalysis in general [147], methanol synthesis has been studied very intensively for several decades by employing a large number of experimental and theoretical techniques. Valuable insights have been gained concerning many interesting aspects of this system. Nevertheless, one of its most fundamental properties,

the precise atomic structure of the catalyst under reaction conditions, is still an open question, although much progress has been made experimentally in recent years, in particular by state-of-the-art imaging techniques like scanning tunneling microscopy [148–152] and transmission electron microscopy [153–156]. Consequently, little is known about the chemical nature and distribution of the active sites, and many contradictory models have been proposed, like Cu^+ dissolved in ZnO [157, 158], metallic copper supported on ZnO [159] and CuZn surface alloys [160–162].

Starting from the NNPs for copper and ZnO, we have constructed the first simple model systems for a CuZnO catalyst in which large copper clusters are adsorbed at the nonpolar ZnO $(10\bar{1}0)$ surface. For this system, we have carried out detailed MD simulations to validate the NNP focusing on the description of the interface between copper and ZnO [163]. We found that even the first preliminary NNPs are able to provide very accurate forces for the interface atoms, while the atoms far from the interface are described with a quality comparable to that of the NNPs for the individual subsystems. Surprisingly, it can thus be concluded that the construction of the NNP for the ternary system is not significantly more challenging than the development of the potentials for the individual subsystems. Still, of course, the chemical complexity is much higher and in total about 100 000 DFT calculations (including the data sets for pure copper and ZnO) were required. Further extensions of the reference set are certainly needed to cover the full relevant configuration space of the ternary system. Still, by employing this preliminary NNP for the CuZnO system it is already possible to carry out MD and MC simulations.

Another system, which we are now studying using high-dimensional NNPs, is water, the most important solvent in chemistry. Consequently, countless potentials have been developed over the decades to study its properties, focussing mainly on the liquid phase [164]. Most of these water force fields have very simple functional forms so they can be used to simulate large systems. They typically contain electrostatic interactions based on fixed point charges and LJ-like effective interactions between the water molecules. For efficiency reasons, often the internal structure of the water molecules is kept rigid. Prominent examples of such potentials are the ST2 [165], SPC [166], TIP3P and TIP4P [167] models.

For a number of applications these simple models do not yield sufficiently accurate results. Consequently, in recent years a lot of effort has been spent on improving these potentials, e.g. by describing polarization [168–171] and by including the internal degrees of freedom of the water molecules explicitly [168, 172]. In particular, Bowman and coworkers have developed very accurate potentials for water clusters, employing a mathematical potential based on permutationally invariant polynomials [54, 56, 60, 173, 174] using high-level coupled cluster calculations.

However, a property that is still common to most water potentials is that they are unable to describe the dissociation and recombination of water molecules, because they are treated as predefined molecular entities. This prevents their application to mechanistic studies of processes involving proton transfers, i.e. to chemical reactions in which water actively participates as a reactant, but also to other systems in which the ability to describe molecular dissociation is essential, e.g. at metal and oxide surfaces. The capability to describe such processes is a mandatory condition for reliable computer simulations of the solid–liquid interface, which is important in many fields of chemistry, e.g. in electrochemistry, corrosion and catalysis.

To date, most water potentials have been developed with specific applications in mind, and the derived potentials are thus not equally applicable to liquid water, small clusters and the rich phase diagram formed by a manifold of ice polymorphs [175]. Carrying out *ab initio* MD simulations of water would overcome this restriction [176–179], but the high computational costs severely limit the system size that can be studied. While for pure water reasonable results can be obtained by employing DFT on-the-fly, simulations of sufficiently extended systems become increasingly challenging if large molecules or surfaces are present.

In order to construct an NNP for water that is equally applicable to flexible and reactive molecules in small clusters, in the bulk liquid and in ice, as a first step we focussed on the development and investigation of a high-dimensional NNP for water clusters of various size [107, 114, 180]. We found that NNPs based on DFT are able to describe the global and local minima correctly in most cases, but it should be noted that for some clusters, in particular for the water hexamer, the energy differences between the local minima are extremely small. Therefore, in such cases the energetic order of the local minima cannot be resolved with confidence even when employing DFT directly, and different functionals may yield slightly different results. An important outcome of our work is, however, that while the binding energies in clusters may differ by up to about 100 meV per monomer depending on the choice of the DFT functional, replacing DFT by an NNP does not introduce significant additional errors [114].

In general, for water the choice of the exchange-correlation functional for constructing the reference set is very important. While the PBE functional [181, 182] typically overestimates the binding energy slightly, the RPBE functional [183] yields binding energies that are too small with respect to coupled cluster data [184]. Both of these well-known phenomena, which are a consequence of the inability of current exchange-correlation functionals to describe dispersion interactions, are also present in the respective NNPs. This can be approximately corrected for the RPBE NNP by the D3 method of Grimme [119], which is directly applicable as discussed in section 3.2. It yields binding energies very close to CCSD(T) data [114]. Currently, work is in progress to extend the validity of the water NNP also to the bulk liquid and a wide range of ice phases. The first very promising results show that structural properties, like radial distribution functions, are very close to DFT data, and also the relative stabilities of different ice polymorphs are in very good agreement with DFT [185].

Other systems that have been studied in detail using NNPs are sodium, to understand the microscopic origins of its anomalous melting behavior under high pressure [186, 187], carbon, to unravel the nucleation mechanism of the direct graphite-to-diamond phase transition [188, 189], and GeTe as

a prototype system for investigating the structural and dynamical properties of phase change materials [190–193], which are important components of rewritable optical storage media and electronic nonvolatile memories.

6. Conclusions

In recent years, the rapid development of mathematical potentials has considerably extended their applicability, and in particular NNPs can now be used to address and solve real chemical problems. The high-dimensional NNP method presented in this work overcomes the restriction to very small systems and can be used to construct very accurate potentials with remaining total energy errors of only a few meV per atom. Further, the uncertainty in energy differences, which are the decisive quantity for successful applications, is even significantly lower. For instance, for the high-pressure phase diagram of silicon, an NNP predicted the relative stabilities of structures that were not included in the training set, with an error of only about 1 meV per atom [136]. This predictive power is not a consequence of the functional form of the NN, but of the large variety of atomic environments included in the training set. Therefore, the composition of the NN training set is of utmost importance for the successful construction of NNPs. For very large systems, which cannot be addressed directly by electronic structure calculations, NNPs can be validated by using the atomic forces as local probes of the PES. The typical error of the NN forces is of the order of 100–200 meV/Bohr with respect to the reference data obtained from first principles. Electrostatic interactions can be included explicitly and without truncation by employing environment-dependent charges, which are fitted to reference charges with an error of about 0.001 e.

In general, NNPs can be constructed using arbitrary reference electronic structure methods, but in practical applications only a few of the available methods are sufficiently efficient to permit the calculation of the thousands or even tens of thousands of training structures that are required to obtain reliable NNPs. Therefore, a natural choice is DFT, which has well-known limitations [194–199]. As by construction an NNP cannot be more accurate than the underlying reference method, this has to be kept in mind when developing NNPs. For some known problems of DFT, like the poor description of van der Waals interactions, correction schemes have been proposed, which can also be used to improve the quality of NNPs.

The most severe disadvantage of NNPs is the effort involved in their construction due to the large number of required training points. This is the price that needs to be paid for their non-physical and highly flexible functional form, which is also the main reason for their numerical accuracy. Procedures have now been developed for constructing the reference data sets almost fully automatically, and situations in which NN predictions are unreliable because the set of reference structures is too sparse are now easy to detect. This is also true for extrapolation, which is a general limitation of all mathematical potentials. Since the region of validity of NNPs can be determined from an analysis of the symmetry functions in the training set, extrapolation is straightforward to identify and therefore does not represent an issue in practical simulations. Still, of course, like all mathematical potentials, NNPs need to be constructed and used with care.

A problem, which has not yet been solved to full satisfaction, is the applicability of NNPs to systems containing a large number of different chemical elements. Being able to address such systems would be important, for instance, for biochemical problems, which require the inclusion of at least six or seven elements. A temporary solution to overcome this limitation for specific applications is to sacrifice the full generality of NNPs, since in biochemical systems like proteins it is generally not necessary to describe the breaking of each bond properly. Instead, NNPs could provide here a useful tool to improve the description of the relevant active sites, which often involve complicated transition metal structures that are difficult to represent by classical force fields. If, on the other hand, full chemical generality is required, because chemical reactions or significant atomic rearrangements could occur at many different places in the system, then high-dimensional NNPs are the method of choice as long as three or four chemical species are sufficient. This includes many questions in materials and surface science, and for these systems NNPs are expected to prove very useful in the near future. If localized chemical processes, e.g. at surfaces, are currently too complex for NNPs, then embedding approaches like a ‘QM/NN’ ansatz might also be an interesting alternative option, which has not yet been explored.

The performance of NNPs is significantly better than that of any electronic structure method. The evaluation by NNPs scales almost linearly with system size in contrast to methods like DFT, which typically exhibit a cubic scaling behavior. For systems that contain about one hundred atoms and are thus routinely accessible by DFT, NNPs are about four to five orders of magnitude more efficient, and this difference becomes even more drastic for larger systems. For very large systems, high-dimensional NNPs are one of the very few methods available for performing MD simulations with an accuracy close to that of electronic structure methods. The effort that needs to be spent on the construction of an NNP is high, but it is paid back quickly in large-scale simulations. On the other hand, NNPs are about two orders of magnitude less efficient than simple classical force fields due to the comparably demanding calculation of the symmetry functions and the evaluation of the nested analytic function of the NN.

Compared to other mathematical potentials, like GAPs [63], which have comparable scopes and limitations, the efficiency of the NNP evaluation does not depend on the size of the underlying reference set, because all information about the topology of the PES is stored in the NN weight parameters. Still, apart from this difference, all mathematical potentials share similar components, like the description of the system by a suitable set of transformed coordinates and the assignment of the energy to the resulting coordinate values. These components can also be combined in a modular way if they have been developed for different approaches. It would be

possible, e.g. to use the four-dimensional spherical harmonics of Bartók *et al* [122] instead of our many-body symmetry functions as NN input variables. Another example, which has been implemented recently, is the combination of permutationally invariant polynomials and NNs [120].

We are convinced that to date only a tiny fraction of the wealth of knowledge about NNs and other machine learning methods, which is available in the computer science community, has been transferred and applied to chemistry and the representation of PESs. Consequently many interesting methodical improvements are to be expected in the years to come, making the development of mathematical potentials an exciting field of research.

Acknowledgments

Financial support by the Deutsche Forschungsgemeinschaft (Emmy Noether program and Cluster of Excellence RESOLV, EXC 1069) is gratefully acknowledged.

References

[1] Allen M P and Tildesley D J 2006 *Computer Simulation of Liquids* (Oxford: Oxford University Press)
[2] Rapaport D C 2013 *The Art of Molecular Dynamics Simulations* 2nd edn (Cambridge: Cambridge University Press)
[3] Frenkel D and Smit B 2001 *Understanding Molecular Simulation: From Algorithms to Applications* 2nd edn (New York: Academic)
[4] Landau D P and Binder K 2009 *A Guide to Monte Carlo Simulations in Statistical Physics* 3rd edn (Cambridge: Cambridge University Press)
[5] Car R and Parrinello M 1985 *Phys. Rev. Lett.* **55** 2471–4
[6] Marx D and Hutter J 2009 *Ab Initio Molecular Dynamics: Basic Theory and Advanced Methods* (Cambridge: Cambridge University Press)
[7] Parr R G and Yang W 1989 *Density Functional Theory of Atoms and Molecules* (Oxford: Oxford University Press)
[8] Koch W and Holthausen M C 2001 *A Chemist's Guide to Density Functional Theory* 2nd edn (New York: Wiley-VCH)
[9] Born M and Oppenheimer R 1927 *Ann. Phys.* **389** 457–84
[10] Truhlar D G, Steckler R and Gordon M S 1987 *Chem. Rev.* **87** 217–36
[11] Schatz G C 1989 *Rev. Mod. Phys.* **61** 669–88
[12] Hollebeek T, Ho T S and Rabitz H 1999 *Ann. Rev. Phys. Chem.* **50** 537–70
[13] Wales D J, Doye J P K, Miller M A, Mortenson P N and Walsh T R 2000 *Adv. Chem. Phys.* **115** 1–111
[14] Brenner D W 2000 *Phys. Status Solidi* B **217** 23–40
[15] Finnis M 2004 *Prog. Mater. Sci.* **49** 1–18
[16] Stone A J 2008 *Science* **321** 787–9
[17] Behler J 2011 *Phys. Chem. Chem. Phys.* **13** 17930–55
[18] Bartlett R J and Musiał M 2007 *Rev. Mod. Phys.* **79** 291–352
[19] Lyakh D I, Musiał M , Lotrich V F and Bartlett R J 2012 *Chem. Rev.* **112** 182–243
[20] Minsky M and Papert S A 1969 *Perceptrons* (Cambridge, MA: MIT Press)
[21] Pople J A, Head-Gordon M and Raghavachari K 1987 *J. Chem. Phys.* **87** 5968–75
[22] Sutton A P, Finnis M W, Pettifor D G and Ohta Y 1988 *J. Phys. C: Solid State Phys.* **21** 35–66
[23] Colombo L 1998 *Comp. Mater. Sci.* **12** 278–87
[24] Bredow T and Jug K 2005 *Theory Chem. Acc.* **113** 1–14
[25] Hammerschmidt T, Drautz R and Pettifor D G 2009 *Int. J. Mater. Res.* **100** 1479–87
[26] Frauenheim T, Seifert G, Elstner M, Hajnal Z, Jungnickel G, Porezag D, Suhai S and Scholz R 2000 *Phys. Status Solidi* B **217** 41–62
[27] Elstner M 2006 *Theory Chem. Acc.* **116** 316–25
[28] Knaup J M, Hourahine B and Frauenheim T 2007 *J. Phys. Chem.* A **111** 5637–41
[29] Jones J E 1924 *Proc. R. Soc. Lond.* A **106** 463–77
[30] Cornell W D, Cieplak P, Bayly C I, Gould I R, Merz K M Jr , Ferguson D M, Spellmeyer D C, Fox T, Caldwell J W and Kollman P A 1995 *J. Am. Chem. Soc.* **117** 5179–97
[31] van Gunsteren W F, Billeter S R, Eising A A, Hünenberger P H, Krüger P, Mark A E, Scott W R P and Tironi I G 1996 *Biomolecular Simulation: The GROMOS96 Manual and User Guide* (Zürich: Vdf Hochschulverlag AG an der ETH Zürich)
[32] Jorgensen W L, Maxwell D S and Tirado-Rives J 1996 *J. Am. Chem. Soc.* **118** 11225–36
[33] Brooks B R, Bruccoleri R E, Olafson B D, States D J, Swaminathan S and Karplus M 1983 *J. Comput. Chem.* **4** 187–217
[34] Allinger N L, Yuh Y H and Lii J H 1989 *J. Am. Chem. Soc.* **111** 8551–66
[35] Senn H M and Thiel W 2007 *Top. Curr. Chem.* **268** 173–290
[36] Warshel A and Weiss R M 1980 *J. Am. Chem. Soc.* **102** 6218–26
[37] Schmitt U W and Voth G A 1998 *J. Phys. Chem.* B **102** 5547–51
[38] Wilhelm F, Schmickler W, Nazmutdinov R R and Spohr E 2008 *J. Phys. Chem.* C **112** 10814–26
[39] van Duin A C T, Dasgupta S, Lorant F and Goddard I I 2001 *J. Phys. Chem.* A **105** 9396–409
[40] Chenoweth K, van Duin A C T and Goddard I I 2008 *J. Phys. Chem. A* **112** 1040 1053 1040–53
[41] Daw M S and Baskes M I 1983 *Phys. Rev. Lett.* **50** 1285–8
[42] Daw M S and Baskes M I 1984 *Phys. Rev.* B **29** 6443–53
[43] Baskes M I 1987 *Phys. Rev. Lett.* **59** 2666–9
[44] Baskes M I, Nelson J S and Wright A F 1989 *Phys. Rev.* B **40** 6085–100
[45] Brenner D W and Garrison B J 1986 *Phys. Rev.* B **34** 1304–7
[46] Brenner D W, Shenderova O A, Harrison J A, Stuart S J, Ni B and Sinnott S B 2002 *J. Phys.: Condens. Matter* **14** 783–802
[47] Tersoff J 1986 *Phys. Rev. Lett.* **56** 632–5
[48] Tersoff J 1988 *Phys. Rev.* B **38** 9902–5
[49] Stillinger F H and Weber T A 1985 *Phys. Rev.* B **31** 5262–71
[50] Coulson C A 1939 *Proc. R. Soc. Lond.* A **169** 413–28
[51] Bishop C M 1996 *Neural Networks for Pattern Recognition* (Oxford: Oxford University Press)
[52] Mitchell T M 1997 *Machine Learning* (New York: McGraw-Hill)
[53] Haykin S 2009 *Neural Networks and Learning Machines* 3rd edn (New York: Pearson)
[54] Braams B J and Bowman J M 2009 *Int. Rev. Phys. Chem.* **28** 577–606
[55] Bowman J M et al 2010 *J. Phys. Chem. Lett.* **1** 1866–74
[56] Wang Y, Shepler B C, Braams B J and Bowman J M 2009 *J. Chem. Phys.* **131** 054511
[57] Brown A, Braams B J, Christoffel K, Jin Z and Bowman J M 2003 *J. Chem. Phys.* **119** 8790–3
[58] McCoy A B, Braams B J, Brown A, Huang X, Jin Z and Bowman J M 2004 *J. Phys. Chem.* A **108** 4991
[59] Huang X, Braams B J, Carter S and Bowman J M 2004 *J. Am. Chem. Soc.* **126** 5042–3
[60] Huang X, Braams B J and Bowman J M 2005 *J. Chem. Phys.* **122** 044308
[61] Sharma A R, Braams B J, Carter S, Shepler B C and Bowman J M 2009 *J. Chem. Phys.* **130** 174301

[62] Shepler B C, Braams B J and Bowman J M 2008 *J. Phys. Chem.* A **112** 9344–51
[63] Bartók A P, Payne M C, Kondor R and Csányi G 2010 *Phys. Rev. Lett.* **104** 136403
[64] Bartók A P, Gillan M J, Manby F R and Csányi G 2013 *Phys. Rev.* B **88** 054104
[65] Mills M J L and Popelier P L A 2012 *Theory Chem. Acc.* **131** 1137
[66] Collins M A 2002 *Theory Chem. Acc.* **108** 313–24
[67] Ischtwan J and Collins M A 1994 *J. Chem. Phys.* **100** 8080–8
[68] Crespos C, Collins M A, Pijper E and Kroes G J 2003 *Chem. Phys. Lett.* **376** 566–75
[69] Crespos C, Collins M A, Pijper E and Kroes G J 2004 *J. Chem. Phys.* **120** 2392–404
[70] Maisuradze G G, Thompson D L, Wagner A F and Minkoff M 2003 *J. Chem. Phys.* **119** 10002–14
[71] Guo Y, Kawano A, Thompson D L, Wagner A F and Minkoff M 2004 *J. Chem. Phys.* **121** 5091–7
[72] Dawes R, Thompson D L, Guo Y, Wagner A F and Minkoff M 2007 *J. Chem. Phys.* **126** 184108
[73] Dawes R, Thompson D L, Wagner A F and Minkoff M 2008 *J. Chem. Phys.* **128** 084107
[74] Makarov D E and Metiu H 1998 *J. Chem. Phys.* **108** 590–598
[75] Ripley B D 2009 *Pattern Recognition and Neural Networks* (Cambridge: Cambridge University Press)
[76] Gasteiger J and Zupan J 1993 *Angew. Chem. Int. Edn Engl.* **32** 503–27
[77] Blank T B, Brown S D, Calhoun A W and Doren D J 1995 *J. Chem. Phys.* **103** 4129–37
[78] McCulloch W and Pitts W 1943 *Bull. Math. Biophys.* **5** 115–33
[79] Rosenblatt F 1958 *Psych. Rev.* **65** 386–408
[80] Werbos P J 1974 Beyond regression: new tools for prediction and analysis in the behavioral sciences *PhD Thesis* Harvard University
[81] Little W A 1974 *Math. Biosci.* **19** 101–20
[82] Cybenko G 1989 *Math. Control Signals Syst.* **2** 303–14
[83] Hornik K, Stinchcombe M and White H 1989 *Neural Netw.* **2** 359–66
[84] Zupan J and Gasteiger J 1991 *Anal. Chim. Acta* **248** 1–30
[85] http://webofknowledge.com
[86] Thomsen J U and Meyer B 1989 *J. Magn. Reson.* **84** 212–7
[87] So S S and Karplus M 1996 *J. Med. Chem.* **39** 1521–30
[88] Handley C M and Popelier P L A 2010 *J. Phys. Chem.* A **114** 3371–83
[89] Behler J 2010 *Chem. Modelling* **7** 1–41
[90] Kohonen T 1988 *Neural Netw.* **1** 3–16
[91] Aspeslagh K 2000 Utilizing a genetic algorithm to search the structure-space of artificial neural networks for optimal architectures *PhD Thesis* Wheaton College, Norton, USA
[92] Raff L M, Komanduri R, Hagan M and Bukkapatnam S T S 2012 *Neural Networks in Chemical Reaction Dynamics* (Oxford: Oxford University Press)
[93] Manzhos S and Carrington T Jr 2006 *J. Chem. Phys.* **125** 194105
[94] Manzhos S, Wang X, Dawes R and Carrington T Jr 2006 *J. Phys. Chem.* A **110** 5295–304
[95] Manzhos S and Carrington T Jr 2007 *J. Chem. Phys.* **127** 014103
[96] Manzhos S and Carrington T Jr 2008 *J. Chem. Phys.* **129** 224104
[97] Manzhos S, Yamashita K and Carrington T Jr 2009 *Comput. Phys. Commun.* **180** 2002–12
[98] Malshe M, Narulkar R, Raff L M, Hagan M, Bukkapatnam S, Agrawal P M and Komanduri R 2009 *J. Chem. Phys.* **130** 184102
[99] Hobday S, Smith R and Belbruno J 1999 *Modelling Simul. Mater. Sci. Eng.* **7** 397–412
[100] Hobday S, Smith R and BelBruno J 1999 *Nucl. Instrum. Methods Phys. Res.* B **153** 247–63
[101] Bholoa A, Kenny S D and Smith R 2007 *Nucl. Instrum. Methods Phys. Res.* B **255** 1–7
[102] Sanville E, Bholoa A, Smith R and Kenny S D 2008 *J. Phys.: Condens. Matter* **20** 285219
[103] Behler J and Parrinello M 2007 *Phys. Rev. Lett.* **98** 146401
[104] Behler J 2011 *J. Chem. Phys.* **134** 074106
[105] Mayer I 2006 *Phys. Chem. Chem. Phys.* **8** 4630–46
[106] Artrith N, Morawietz T and Behler J 2011 *Phys. Rev.* B **83** 153101
[107] Morawietz T, Sharma V and Behler J 2012 *J. Chem. Phys.* **136** 064103
[108] Ewald P P 1921 *Ann. Phys.* **64** 253–87
[109] Hirshfeld F L 1977 *Theory Chim. Acta* **44** 129–38
[110] Houlding S, Liem S Y and Popelier P L A 2007 *Int. J. Quantum Chem.* **107** 2817–27
[111] Darley M G, Handley C M and Popelier P L A 2008 *J. Chem. Theory Comput.* **4** 1435–48
[112] Handley C M and Popelier P L A 2009 *J. Chem. Theory Comput.* **5** 1474–89
[113] Handley C M, Hawe G I, Kell D B and Popelier P L A 2009 *Phys. Chem. Chem. Phys.* **11** 6365–76
[114] Morawietz T and Behler J 2013 *J. Phys. Chem.* A **117** 7356–66
[115] von Lilienfeld O A, Tavernelli I, Rothlisberger U and Sebastiani D 2004 *Phys. Rev. Lett.* **93** 153004
[116] Dion M, Rydberg H, Schröder E, Langreth D C and Lundqvist B I 2004 *Phys. Rev. Lett.* **92** 246401
[117] Grimme S 2006 *J. Comput. Chem.* **27** 1787–99
[118] Tkatchenko A and Scheffler M 2009 *Phys. Rev. Lett.* **102** 073005
[119] Grimme S, Antony J, Ehrlich S and Krieg H 2010 *J. Chem. Phys.* **132** 154104
[120] Li J, Jiang B and Guo H 2013 *J. Chem. Phys.* **139** 204103
[121] Rupp M, Tkatchenko A, Müller K R and von Lilienfeld O A 2012 *Phys. Rev. Lett.* **108** 058301
[122] Bartók A P, Kondor R and Csányi G 2013 *Phys. Rev.* B **87** 184115
[123] Behler J, Lorenz S and Reuter K 2007 *J. Chem. Phys.* **127** 014705
[124] Gassner H, Probst M, Lauenstein A and Hermansson K 1998 *J. Phys. Chem.* A **102** 4596–605
[125] Jovan Jose K V, Artrith N and Behler J 2012 *J. Chem. Phys.* **136** 194111
[126] Geiger P and Dellago C 2013 *J. Chem. Phys.* **139** 164105
[127] Steinhardt P J, Nelson D R and Ronchetti M 1983 *Phys. Rev.* B **28** 784 –805
[128] Martoňák R, Laio A and Parrinello M 2003 *Phys. Rev. Lett.* **90** 75503
[129] Skinner A J and Broughton J Q 1995 *Modelling Simul. Mater. Sci. Eng.* **3** 371–90
[130] Rumelhart D E, Hinton G E and Williams R J 1986 *Nature* **323** 533–6
[131] Witkoskie J B and Doren D J 2005 *J. Chem. Theory Comput.* **1** 14–23
[132] Shah S, Palmieri F and Datum M 1992 *Neural Netw.* **5** 779–87
[133] Blank T B and Brown S D 1994 *J. Chemom.* **8** 391–407
[134] Press W H, Teukolsky S A, Vetterling W T and Flannery B P 2007 *Numerical Recipes: The Art of Scientific Programming* 3rd edn (Cambridge: Cambridge University Press)
[135] Siddique M N H and Tokhi M O 2001 *Int. Jt. Conf. Neural Netw. Proc.* **4** 2673
[136] Behler J, Martoňák R, Donadio D and Parrinello M 2008 *Phys. Rev. Lett.* **100** 185501
[137] Behler J, Martoňák R, Donadio D and Parrinello M 2008 *Phys. Status Solidi* B **245** 2618–29

[138] Mujica A, Rubio A, Muñoz A and Needs R J 2003 *Rev. Mod. Phys.* **75** 863–912
[139] Justo J F, Bazant M Z, Kaxiras E, Bulatov V V and Yip S 1998 *Phys. Rev.* B **58** 2539–50
[140] Bazant M Z, Kaxiras E and Justo J F 1997 *Phys. Rev.* B **56** 8542–52
[141] Wang C Z, Pan B C and Ho K M 1999 *J. Phys.: Condens. Matter* **11** 2043–9
[142] Lenosky T J, Sadigh B, Alonso E, Bulatov V V, de la Rubia T D, Kim J, Voter A F and Kress J D 2000 *Modelling Simul. Mater. Sci. Eng.* **8** 825–41
[143] Erhart P and Albe K 2005 *Phys. Rev.* B **71** 35211
[144] Gillespie B A, Zhou X W, Murdick D A, Wadley H N G, Drautz R and Pettifor D G 2007 *Phys. Rev.* B **75** 155207
[145] Laio A and Parrinello M 2002 *Proc. Natl. Acad. Sci.* **99** 12562–6
[146] Artrith N and Behler J 2012 *Phys. Rev.* B **85** 045439
[147] Bäumer M and Freund H J 1999 *Prog. Surf. Sci.* **61** 127–98
[148] Dulub O, Boatner L A and Diebold U 2002 *Surf. Sci.* **504** 271–81
[149] Vogel Koplitz L, Dulub O and Diebold U 2003 *J. Phys. Chem.* B **107** 10583–90
[150] Dulub O, Batzill M and Diebold U 2005 *Top. Catal.* **36** 65–76
[151] Kroll M and Köhler U 2007 *Surf. Sci.* **601** 2182–8
[152] Kroll M, Löber T, Schott V, Wöll C and Köhler U 2012 *Phys. Chem. Chem. Phys.* **14** 1654–9
[153] Hansen P L, Wagner J B, Helveg S, Rostrup-Nielsen J R, Clausen B S and Topsøe H 2002 *Science* **295** 2053–5
[154] Kasatkin I, Kniep B and Ressler T 2007 *Phys. Chem. Chem. Phys.* **9** 878–83
[155] Kasatkin I, Kurr P, Kniep B, Trunschke A and Schlögl R 2007 *Angew. Chem. Int. Edn Engl.* **119** 7465–8
[156] Kurr P, Kasatkin I, Girgsdies F, Trunschke A, Schlögl R and Ressler T 2008 *Appl. Catal. A* **348** 153–64
[157] Ponec V 1992 *Surf. Sci.* **272** 111–7
[158] Harikumar K R and Rao C N R 1998 *Appl. Surf. Sci.* **125** 245–9
[159] Clausen B S, Lengeler B and Rasmussen B S 1985 *J. Phys. Chem.* **89** 2319–24
[160] Fujitani T and Nakamura J 2000 *Appl. Catal.* A **191** 111–29
[161] Choi Y, Futagami K, Fujitani T and Nakamura J 2001 *Appl. Catal.* A **208** 163–7
[162] Behrens M et al 2012 *Science* **336** 893–7
[163] Artrith N, Hiller B and Behler J 2013 *Phys. Status Solidi* B **250** 1191–203
[164] Guillot B 2002 *J. Mol. Liq.* **101** 219–60
[165] Stillinger F H and Rahman A 1974 *J. Chem. Phys.* **60** 1545 –57
[166] Berendsen H J C, Postma J P M, van Gunsteren W F and Hermans J 1981 *Intermolecular Forces* (Dordrecht: Reidel)
[167] Jorgensen W L, Chandrasekhar J, Madura J D, Impey R W and Klein M L 1983 *J. Chem. Phys.* **79** 926–35
[168] Burnham C J and Xantheas S S 2002 *J. Chem. Phys.* **116** 5115–24
[169] Halley J W, Rustad J R and Rahman A 1993 *J. Chem. Phys.* **98** 4110–9
[170] Baranyai A 2009 *J. Mol. Liq.* **148** 88–93
[171] Brodholt J, Sampoli M and Vallauri R 1995 *Mol. Phys.* **86** 149–58
[172] Toukan K and Rahman A 1985 *Phys. Rev.* B **31** 2643–8
[173] Huang X, Braams B J and Bowman J M 2006 *J. Phys. Chem.* A **110** 445 451 445–51
[174] Wang Y and Bowman J M 2010 *Chem. Phys. Lett.* **491** 1–10
[175] Bartels-Rausch T et al 2012 *Rev. Mod. Phys.* **84** 885–944
[176] Laasonen K, Sprik M, Parrinello M and Car R 1993 *J. Chem. Phys.* **99** 9080–9
[177] Izvekov S and Voth G A 2002 *J. Chem. Phys.* **116** 10372–6
[178] Marx D 2006 *Chem. Phys. Chem.* **7** 1848–70
[179] Lee H S and Tuckerman M E 2007 *J. Chem. Phys.* **126** 164501
[180] Morawietz T and Behler J 2013 *Z. Phys. Chem.* **227** 1559–81
[181] Perdew J P, Burke K and Ernzerhof M 1996 *Phys. Rev. Lett.* **77** 3865–8
[182] Perdew J P, Burke K and Ernzerhof M 1997 *Phys. Rev. Lett.* **78** 1396
[183] Hammer B, Hansen L B and Nørskov J K 1999 *Phys. Rev.* B **59** 7413–21
[184] Temelso B, Archer K A and Shields G C 2011 *J. Phys. Chem.* A **115** 12034–46
[185] Morawietz T and Behler J unpublished results
[186] Eshet H, Khaliullin R Z, Kühne T D, Behler J and Parrinello M 2010 *Phys. Rev.* B **81** 184107
[187] Eshet H, Khaliullin R Z, Kühne T D, Behler J and Parrinello M 2012 *Phys. Rev. Lett.* **108** 115701
[188] Khaliullin R Z, Eshet H, Kühne T D, Behler J and Parrinello M 2010 *Phys. Rev.* B **81** 100103
[189] Khaliullin R Z, Eshet H, Kühne T D, Behler J and Parrinello M 2011 *Nature Mater.* **10** 693–7
[190] Sosso G C, Miceli G, Caravati S, Behler J and Bernasconi M 2012 *Phys. Rev.* B **85** 174103
[191] Sosso G C, Donadio D, Caravati S, Behler J and Bernasconi M 2012 *Phys. Rev.* B **86** 104301
[192] Sosso G C, Behler J and Bernasconi M 2012 *Phys. Status Solidi* B **249** 1880–5
[193] Sosso G C, Miceli G, Caravati S, Giberti F, Behler J and Bernasconi M 2013 *J. Phys. Chem. Lett.* **4** 4241–6
[194] Feibelman P J, Hammer B, Nørskov J K, Wagner F, Scheffler M, Stumpf R, Watwe R and Dumesic J 2001 *J. Phys. Chem.* B **105** 4018–25
[195] Paier J, Marsman M and Kresse G 2007 *J. Chem. Phys.* **127** 024103
[196] Cohen A J, Mori-Sánchez P and Yang W 2008 *Science* **321** 792–4
[197] Cohen A J, Mori-Sánchez P and Yang W 2011 *Chem. Rev.* **112** 289–320
[198] Ruzsinszky A and Perdew J P 2011 *Comput. Theory Chem.* **963** 2–6
[199] Steinmann S N, Piemontesi C, Delachat A and Corminboeuf C 2012 *J. Chem. Theory Comput.* **8** 1629–40
[200] Tafeit E, Estelberger W, Horejsi R, Moeller R, Oettl K, Vrecko K and Reibnegger G 1996 *J. Mol. Graph.* **14** 12–8
[201] Brown D F R, Gibbs M N and Clary D C 1996 *J. Chem. Phys.* **105** 7597–604
[202] No K T, Chang B H, Kim S Y, Jhon M S and Scheraga H A 1997 *Chem. Phys. Lett.* **271** 152–6
[203] Prudente F V and Soares Neto J J 1998 *Chem. Phys. Lett.* **287** 585–9
[204] Prudente F V, Acioli P H and Soares Neto J J 1998 *J. Chem. Phys.* **109** 8801–8
[205] Cho K W, No K T and Scheraga H A 2002 *J. Mol. Struct.* **641** 77–91
[206] Rocha Filho T M, Oliveira Z T Jr , Malbouisson L A C, Gargano R and Soares Neto J J 2003 *Int. J. Quantum Chem.* **95** 281–8
[207] Bittencourt A C P, Prudente F V and Vianna J D M 2004 *Chem. Phys.* **297** 153–61 153–61
[208] Raff L M, Malshe M, Hagan M, Doughan D, Rockley M and Komanduri R 2005 *J. Chem. Phys.* **122** 084104
[209] Agrawal P M, Raff L M, Hagan M T and Komanduri R 2006 *J. Chem. Phys.* **124** 134306
[210] Malshe M, Narulkar R, Raff L M, Hagan M, Bukkapatnam S and Komanduri R 2008 *J. Chem. Phys.* **129** 044111
[211] Lee H M and Raff L M 2008 *J. Chem. Phys.* **128** 194310
[212] Malshe M, Raff L M, Rockley M G and Hagan M 2007 *J. Chem. Phys.* **127** 134105

[213] Pukrittayakamee A, Malshe M, Hagan M, Raff L M, Narulkar R, Bukkapatnum S and Komanduri R 2009 *J. Chem. Phys.* **130** 134101
[214] Le H M, Huynh S and Raff L M 2009 *J. Chem. Phys.* **131** 014107
[215] Le H M and Raff L M 2010 *J. Phys. Chem.* A **114** 45–53
[216] Manzhos S, Nakai K and Yamashita K 2010 *Chem. Phys. Lett.* **493** 229–33
[217] Le H M, Dinh T S and Le H V 2011 *J. Phys. Chem.* A **115** 10862–70
[218] Nguyen H T T and Le H M 2012 *J. Phys. Chem.* A **116** 4629–38
[219] Chen J, Xu X, Xu X and Zhang D H 2013 *J. Chem. Phys.* **138** 221104
[220] Chen J, Xu X, Xu X and Zhang D H 2013 *J. Chem. Phys.* **138** 154301
[221] Jiang B and Guo H 2013 *J. Chem. Phys.* **139** 054112
[222] Nguyen-Truong H T, Thi C M and Le H M 2013 *Chem. Phys.* **426** 31–7
[223] Lorenz S, Groß A and Scheffler M 2004 *Chem. Phys. Lett.* **395** 210–5
[224] Behler J, Delley B, Lorenz S, Reuter K and Scheffler M 2005 *Phys. Rev. Lett.* **94** 36104
[225] Behler J, Reuter K and Scheffler M 2008 *Phys. Rev.* B **77** 115421
[226] Lorenz S, Scheffler M and Groß A 2006 *Phys. Rev.* B **73** 115431
[227] Ludwig J and Vlachos D G 2007 *J. Chem. Phys.* **127** 154716
[228] Latino D A R S, Fartaria R P S, Freitas F F M, de Sousa J A and Fernandes F M S S 2008 *J. Electroanal. Chem.* **624** 109–20
[229] Carbogno C, Behler J, Groß A and Reuter K 2008 *Phys. Rev. Lett.* **101** 096104
[230] Carbogno C, Behler J, Reuter K and Groß A 2010 *Phys. Rev.* B **81** 035410
[231] Latino D A R S, Fartaria R P S, Freitas F F M, Aires-De-Sousa J and Silva Fernandes F M S 2010 *Int. J. Quantum Chem.* **110** 432–45
[232] Manzhos S and Yamashita K 2010 *Surf. Sci.* **604** 554–60
[233] Goikoetxea I, Beltrán J, Meyer J, Juaristi J I, Alducin M and Reuter K 2012 *New J. Phys.* **14** 013050
[234] Liu T, Fu B and Zhang D H 2014 *Sci. China Chem.* **57** 147–55